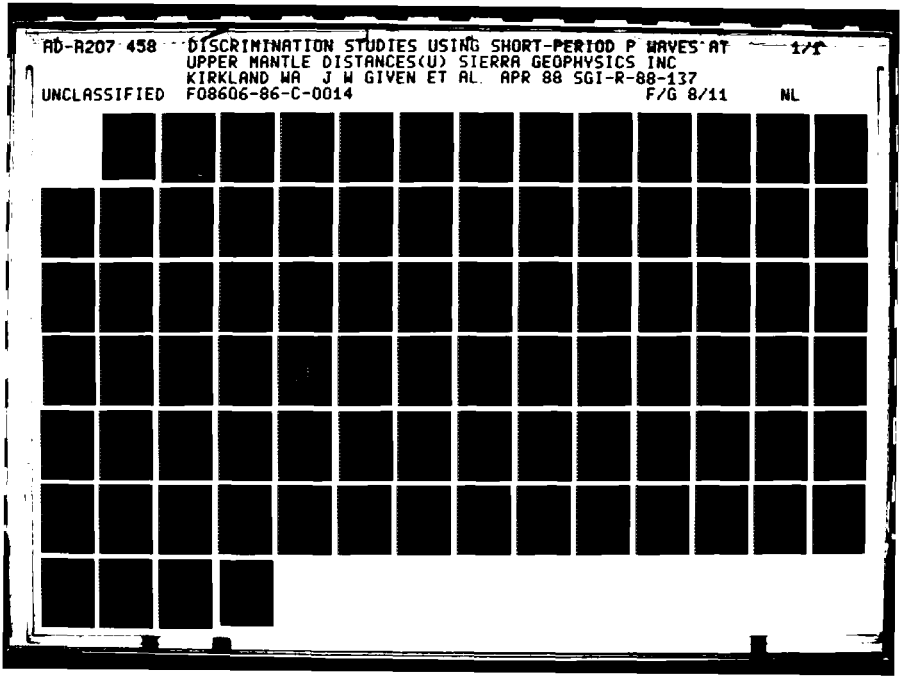
AD-A207 458
DISCRIMINATION STUDIES USING SHORT-PERIOD P WAVES AT
UPPER MANTLE DISTANCES(U) SIERRA GEOPHYSICS INC
KIRKLAND WA J W GIVEN ET AL. APR 88 SGI-R-88-137
UNCLASSIFIED F08606-86-C-0014
F/G 8/11
NL

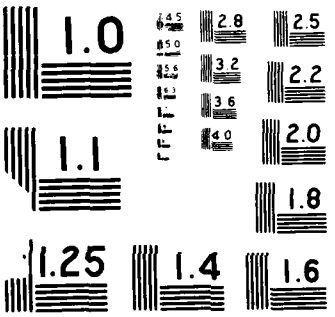
1.0
1.1
1.25
1.4
1.6
1.8
2.0
2.2
2.5
2.8
3.2
3.6
4.0

SGI-R-88-137

DISCRIMINATION STUDIES USING SHORT-PERIOD P WAVES AT UPPER MANTLE DISTANCES

J.W. GIVEN
S.M. IHNEN
G.R. MELLMAN
W.C. TUCKER

SIERRA GEOPHYSICS, INC.
11255 KIRKLAND WAY
KIRKLAND, WASHINGTON 98033

APRIL 1988

FINAL REPORT
JANUARY 1986 - JANUARY 1988

AIR FORCE TECHNICAL APPLICATIONS CENTER/TTR
HEADQUARTERS UNITED STATES AIR FORCE
PATRICK AIR FORCE BASE, FLORIDA 32925

Sierra

SPONSORED BY

DEFENSE ADVANCED RESEARCH PROJECT AGENCY (DoD)

AFTAC/TTR
REGIONAL DISCRIMINATION STUDY
ARPA ORDER NO. 4511, AMENDMENT 7
ISSUED BY AFTAC UNDER CONTRACT #F08606-86-C-0014

REPORT DOCUMENTATION PAGE

1a. REPORT SECURITY CLASSIFICATION Unclassified	1b. RESTRICTIVE MARKINGS
2a. SECURITY CLASSIFICATION AUTHORITY	3. DISTRIBUTION/AVAILABILITY OF REPORT Approved for public release; distribution is unlimited.
2b. DECLASSIFICATION/DOWNGRADING SCHEDULE	
4. PERFORMING ORGANIZATION REPORT NUMBER(S) SGI-R-88-137	5. MONITORING ORGANIZATION REPORT NUMBER(S)
6a. NAME OF PERFORMING ORGANIZATION Sierra Geophysics, Inc. — 6b. OFFICE SYMBOL (If applicable) 4R088	7a. NAME OF MONITORING ORGANIZATION Air Force Technical Applications Center/TTR
6c. ADDRESS (City, State and ZIP Code) 11255 Kirkland Way Kirkland, WA 98033	7b. ADDRESS (City, State and ZIP Code) Headquarters United States Air Force Patrick Air Force Base, FL 32925
8a. NAME OF FUNDING/SPONSORING ORGANIZATION Defense Advanced Research Projects Agency — 8b. OFFICE SYMBOL (If applicable) NMRO	9. PROCUREMENT INSTRUMENT IDENTIFICATION NUMBER F08606-86-C-0014
8c. ADDRESS (City, State and ZIP Code) 1400 Wilson Boulevard Arlington, VA 22209	10. SOURCE OF FUNDING NOS. PROGRAM ELEMENT NO.: 62714E — PROJECT NO.: DT6121 — TASK NO.: 3.1, 3.2 — WORK UNIT NO.:
11. TITLE (Include Security Classification) See Section 16	
12. PERSONAL AUTHOR(S) J.W. Given, S.M. Ihnen, G.R. Mellman, W.C. Tucker	
13a. TYPE OF REPORT Final — 13b. TIME COVERED FROM Jan.'86 TO Jan.'88	14. DATE OF REPORT (Yr., Mo., Day) 1988 January — 15. PAGE COUNT 77
16. SUPPLEMENTARY NOTATION Discrimination Studies Using Short-Period P Waves at Upper Mantle Distances	
17. COSATI CODES: FIELD / GROUP / SUB. GR.	18. SUBJECT TERMS (Continue on reverse if necessary and identify by block number) Discrimination, earthquake, explosion, upper mantle structure, Pearce processor

19. ABSTRACT (Continue on reverse if necessary and identify by block number)

Explosion seismograms recorded at upper mantle distances in northwest Eurasia are examined for the purpose of characterizing their time domain signature and determining the effectiveness of a Pearce algorithm discrimination scheme at these distances. The amplitude and timing of the major P-wave branches in the distance range 500 to 4000 km are predictable in terms of some simple published upper mantle velocity models. The signature of the explosion seismograms is then compared to predicted earthquake seismograms, using a double couple at depth model for the earthquake, to estimate the discrimination potential of this data. In most cases, an explosion should be distinguishable from an earthquake at depths greater than 15 km, given several azimuthally well-distributed stations.

Theoretical modeling using complete synthetic seismograms for proposed P- and S-wave velocity structures and attenuation models indicate that the P-wave amplitudes remain nearly constant from 800 to 3000 km and are a factor of 3 larger than the amplitudes predicted at teleseismic distances.

20 DISTRIBUTION/AVAILABILITY OF ABSTRACT UNCLASSIFIED/UNLIMITED ☒ SAME AS RPT. ☐ DTIC USERS ☐	21. ABSTRACT SECURITY CLASSIFICATION Unclassified
22a. NAME OF RESPONSIBLE INDIVIDUAL Capt. Donald A. Hirst	22b. TELEPHONE NUMBER (Include Area Code) (407) 494-5263 — 22c. OFFICE SYMBOL AFTAC/TTR

Between 2000 and 25000 km the waveforms are very complex, due to the presence of 5 major P-wave arrivals in the first 10 s. Beyond 3000 km the first arrival is small relative to a large coda apparently caused by scattering off the ends of the 400 and 700 km discontinuities.

We interpret later arrivals in the coda of the seismograms as either upper mantle arrival branches or depth phases from earthquakes. If a large phase arrives outside of some time window in which an upper mantle P arrival is expected, then it is interpreted to be a depth phase from an earthquake. About 90% of the available explosion seismograms do not have dominant arrivals outside of the predicted windows. Forty-five percent of a sample of earthquake seismograms have large arrivals in addition to the upper mantle phases. The earthquake data is, however, from single station data and such an approach will require data at several different azimuths.

We tested some waveform processing methods to enhance the detection of later phases that are consistent between stations. In some cases, a spiking filter applied to the auto-correlation of the seismograms enabled us to isolate the depth phases when several stations at different distances and azimuths from an event could be compared and stacked. A much more difficult problem is the determination of the polarity of the later arrivals; due to the high amplitude of the coda, the signal to noise ratio for these arrivals is not sufficient to estimate polarity.

TABLE OF CONTENTS

LIST OF FIGURES

1.0 Summary

Explosion seismograms recorded at upper mantle distances in northwest Eurasia are examined for the purpose of characterizing their time domain signature and determining the effectiveness of a Pearce algorithm discrimination scheme at these distances. The amplitude and timing of the major P-wave branches in the distance range 500 to 4000 km are predictable in terms of some simple published upper mantle velocity models. The signature of the explosion seismograms is then compared to predicted earthquake seismograms, using a double couple at depth model for the earthquake, to estimate the discrimination potential of this data. In most cases, an explosion should be distinguishable from an earthquake at depths greater than 15 km, given several azimuthally well-distributed station.

Theoretical modeling using complete synthetic seismograms for proposed P- and S-wave velocity structures and attenuation models indicate that the P-wave amplitudes remain nearly constant from 800 to 3000 km and are a factor of 3 larger than the amplitudes predicted at teleseismic distances. Between 2000 and 2500 km the waveforms are very complex, due the presence of 5 major P-wave arrivals in the first 10 s. Beyond 3000 km the first arrival is small relative to a large coda apparently caused by scattering off the ends of the 400 and 700 km discontinuities.

We interpret later arrivals in the coda of the seismograms as either upper mantle arrival branches or depth phases from earthquakes. If a

large phase arrives outside of some time window in which an upper mantle P arrival is expected, then it interpreted to be a depth phase from an earthquake. About 90% of the available explosion seismograms do not have dominant arrivals outside of the predicted windows. Forty-five percent of a sample of earthquake seismograms have large arrivals in addition to the upper mantle phases. The earthquake data is, however, from single station data and such an approach will require data at several different azimuths.

We tested some waveform processing methods to enhance the detection of later phases that are consistent between stations. In some cases, a spiking filter applied to the autocorrelation of the seismograms enabled us to isolate the depth phases when several stations at different distances and azimuths from an event could be compared and stacked. A much more difficult problem is the determination of the polarity of the later arrivals; due to the high amplitude of the coda, the signal to noise ratio for these arrivals is not sufficient to estimate polarity.

2.0 Introduction

Seismic body waves at distances less than 3000 km are very complex due to strong vertical heterogeneity in the upper mantle velocity structure. At least three major velocity discontinuities between the surface and 700 km produce multiple P (and S) wave arrivals throughout this distance range. The complexity introduced into the seismograms due to structure obscures many of the details of the source processes, and data in this distance range have been largely ignored for the purposes of detailed source modeling. However, in order to monitor small underground nuclear tests, it is important to know if the structural effects can be sufficiently calibrated so that source parameters useful for discrimination can be resolved. In the following report, we will be concerned with analyzing P-wave data from 700 to 3000 km in northern Europe and western Russia to isolate those features in the seismograms that can be related to the depth and radiation pattern of a seismic event, which in turn can be used for discrimination.

When underground testing of nuclear explosions began, it was noticed that seismograms from explosions were much simpler than seismograms from earthquakes (Douglas, 1966, 1981). However, straightforward characterization of the complexity of a wavetrain did not turn out to be a useful discriminant since some earthquakes looked like explosions and seismograms from explosions showed some puzzling complexities

(Thirlaway, 1967). With the discovery of the m_b - M_S discriminant, complexity as a simple parameter ceased to be of much interest as a discriminant. However, there remains considerable interest in modeling the complexity observed in seismograms in terms of well understood phenomena and interpreting the results in the context of discrimination. Two characteristics of the earthquake and explosion sources lend themselves to modeling: the source depth and the focal mechanism.

The depth of earthquakes, typically greater than 3 km, introduces complexity into the seismograms due to the later arriving reflections of the body waves from the free surface. An explosion is usually close enough to the surface that the separation between P and pP is less than a second. Furthermore, an earthquake generates substantial S waves; the maximum S-wave amplitude is a factor of 4 to 5 larger than the maximum P-wave amplitude. The S waves can reflect from the free surface and other near-source heterogeneities adding to the complex appearance of the seismogram. In addition, an earthquake has a radiation pattern that causes the appearance of the seismograms, in particular the relative amplitude of the later arriving phases, to vary with azimuth and distance.

Thus, earthquakes should, for a variety of reasons, produce seismograms that are very different in appearance from explosions. The differences should become more evident when seismograms from several stations are compared and systematic similarities and

differences are explored. A typical example of this kind of analysis is the routine processing of pP observations to obtain depth. The pP - P time and the sP - P times should systematically decrease with distance from an event. Observing this "step-out" is a usual way of confirming the identification of a particular phase as a surface reflection.

Pearce (1977, 1979, 1980) developed an algorithm for using the relative amplitudes of the P, pP, and sP phases recorded on a seismogram, in addition to the standard measurements of polarity, as constraints in determining earthquake focal mechanisms. This technique has attracted attention as a discrimination tool since it provides a framework for interpreting a suite of seismograms from an event in terms of a physical model in which earthquakes and explosions are fundamentally different. Furthermore, the method uses relative amplitudes and can, in principle, provide valuable constraints on the source mechanism with fewer stations and poorer signal quality than is required by the traditional methods that use polarity. McLaughlin et al. (1983, 1985) implemented the technique to test its usefulness as a discrimination tool. Subsequent work by those authors has extended the method to provide an estimate of the likelihood of a particular mechanism, which is valuable to formally compare different interpretations of the same data.

McLaughlin et al. (1983) found that there was a certain minimum complexity expected in a group ot seismograms that are azimuthally well distributed around an earthquake. With four or more stations

recording the event, they found that it was probable that pP or sP would be a dominant phase (larger than the P wave) on at least one record. This suggests that by simply observing the amplitude of the P-wave coda relative to the P wave at several azimuths sufficient constraints can be placed on the amplitudes of the surface reflections, pP and sP, to confirm that the event was either an explosion or a very shallow earthquake.

The Pearce algorithm can detect when a set of seismograms are incompatible with a double couple mechanism, but it is very difficult to unambiguously determine an event to be an earthquake, since methods of detonating multiple explosions to simulate earthquakes are conceivable. For better constraints on the source process, it is desirable to have absolute polarity information for the initial and later arrivals. Large dilatational arrivals will probably be associated with an earthquake. Polarities are usually read by observing the first motion of a phase, which requires a good signal to noise ratio over a broad frequency band. Determining the polarity of phases arriving in the coda of the initial P wave is often very difficult. Smart and McLaughlin (1985) have developed a correlation technique to determine the relative polarities of the P and pP waves for all seismograms from a network to determine consistent polarity readings for all stations recording an event. The results can be used in addition to the relative amplitude data in the Pearce processor, or as input to a simple first motion focal plane method. This method appears to show some promise for events with clearly defined depth

phase arrivals, however it is difficult to assess its performance in cases of low signal level or complex waveforms.

Most of these tools for analyzing body wave seismograms for determining probable source mechanisms are useful only in the distance range from 3000 to 10000 km where the propagation effects are reasonably homogeneous and well known throughout the world. To apply these methods to small events, we need to use seismograms that are closer to the source. Aside from the obvious increase in amplitude due to simply being nearer the source, the velocity gradients in the uppermost 700 km are larger than in the deeper mantle and this feature has a tendency to further enhance the amplitudes of the P waves due to focusing. The amplitude increase is often offset by high attenuation in the uppermost mantle; however, for stable continental paths, the Q in the uppermost mantle is high enough to still anticipate an appreciable amplitude enhancement in data at distances less than 3000 km.

The purpose of our research is to investigate wave propagation at distances of less than 3000 km to see if the features in the seismograms relating to source depth and fault mechanism can be reliably detected for the purposes of discrimination. We are particularly interested in whether the techniques that are promising at teleseismic distances can be applied at upper mantle distances. In a previous report (Given et al., 1987) we reviewed the general features of wave propagation in northern Europe and the western Soviet Union and concluded that many of these features could be attributed to

the upper mantle structure and, more importantly, could be predicted on the basis of the results of previous studies on the velocity structure. For the explosions that we observed, there were few surprises in the form of large later arrivals that did not correspond to predicted arrivals from some simple models of the P-wave velocity structure. However, as expected, the P- wave coda from simple explosions is energetic compared to what is typically observed on explosion seismograms at teleseismic distances and determining the amplitude and polarity of later arrivals will be more difficult. Nevertheless, we determined that if we could constrain the surface reflections to be smaller than a maximum coda amplitude that is smaller than the direct P at a minimum of four stations with good azimuthal coverage, then the observed seismograms are incompatible with an earthquake source. However, because of uncertainties in the relative arrival times of the different P-wave branches, the minimum depth of events for which this may be a useful discrimination tool is between 10 and 15 km. In our previous report we also introduced some correlation techniques to enhance the observability of the depth phases and determine the relative polarity.

In the following report, we will present more information pertaining to the propagation characteristics of northwest Eurasia. We have completed a modeling study to determine the amplitude enhancement we should expect at the upper mantle ranges if current models of attenuation are taken into account. We will show a preliminary assessment of how well some complexity measurements, when interpreted by a Pearce processor, or similar algorithm, can separate earthquakes

and explosions. We will present more results on applying a correlation method to detect depth phases in actual data.

3.0 Characteristics of P-Wave Seismograms at Upper Mantle Distances in Northwest Eurasia

At distances less than 30^{o}, the P waves are made up of as many as five separate arrivals, due to the vertical velocity heterogeneity in the upper mantle. If a source signature, diagnostic of the source depth of mechanism, is to be extracted from these phases, the timing and relative amplitudes of the upper mantle arrivals must be predictable. As a preliminary to devising any strategy for using these waveforms to constrain source parameters, we will examine the predictability of seismograms at these distances. In our previous report, (Given et al., 1987) we presented a review of the pertinent observations that can be used to characterize seismograms recorded at the regional to upper mantle distances (500 - 3500 km). In the following, we will briefly summarize the results of that discussion.

Figure 1 presents a travel time curve for a particularly simple velocity model, KCA, derived from observations at the NORSAR array by King and Calcagnile (1976). Since model KCA was derived to predict only the travel time and apparent velocity data, we must characterize the general amplitude and waveform behavior even if only in some qualitative way. One way is to derive a more complex velocity model that also fits the amplitudes, such as model K8 (Given and Helmberger, 1980) as discussed in the previous report. Instead, we will present a semi-quantitative characterization of the amplitude behavior of the various P-wave branches as labeled in Figure 1. Figure 2 shows the

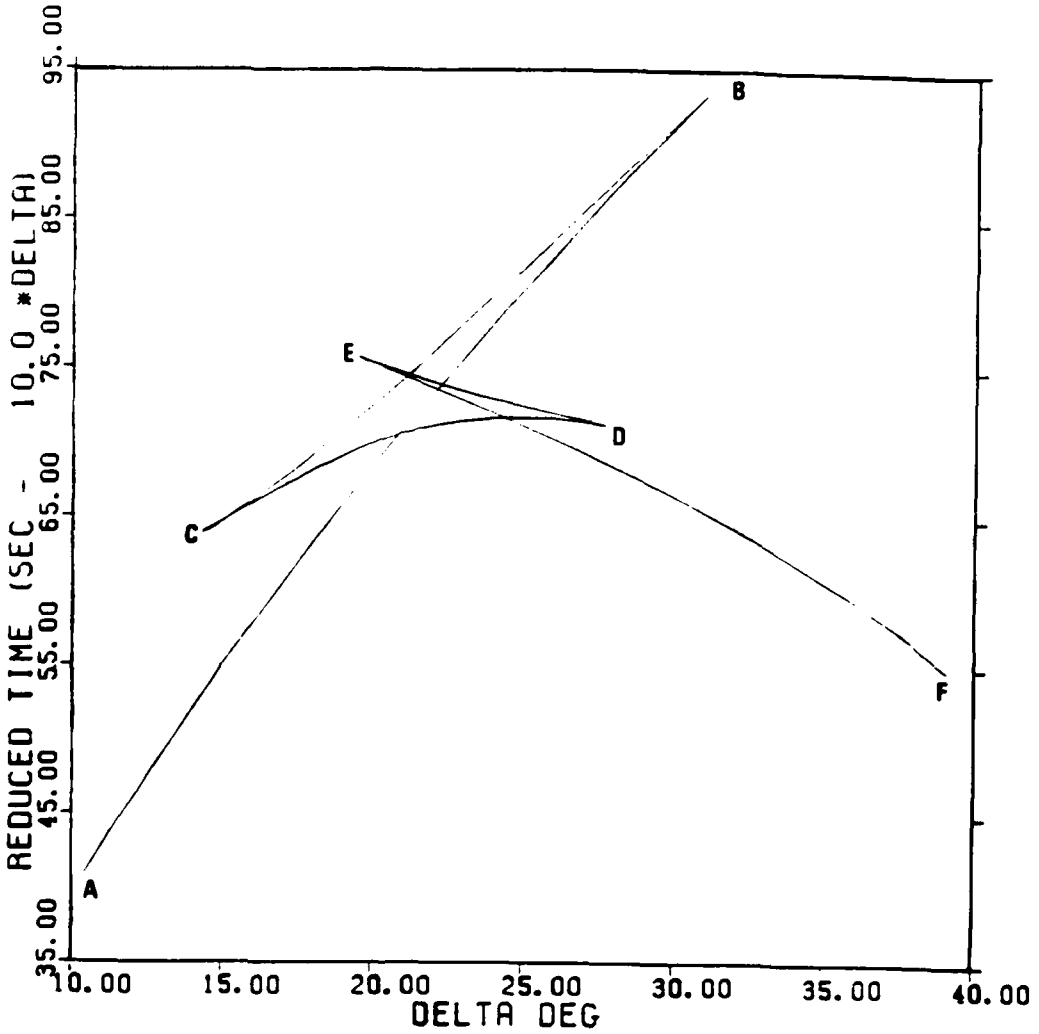

Figure 1. Travel time curve for the upper mantle models for northwest Eurasia.

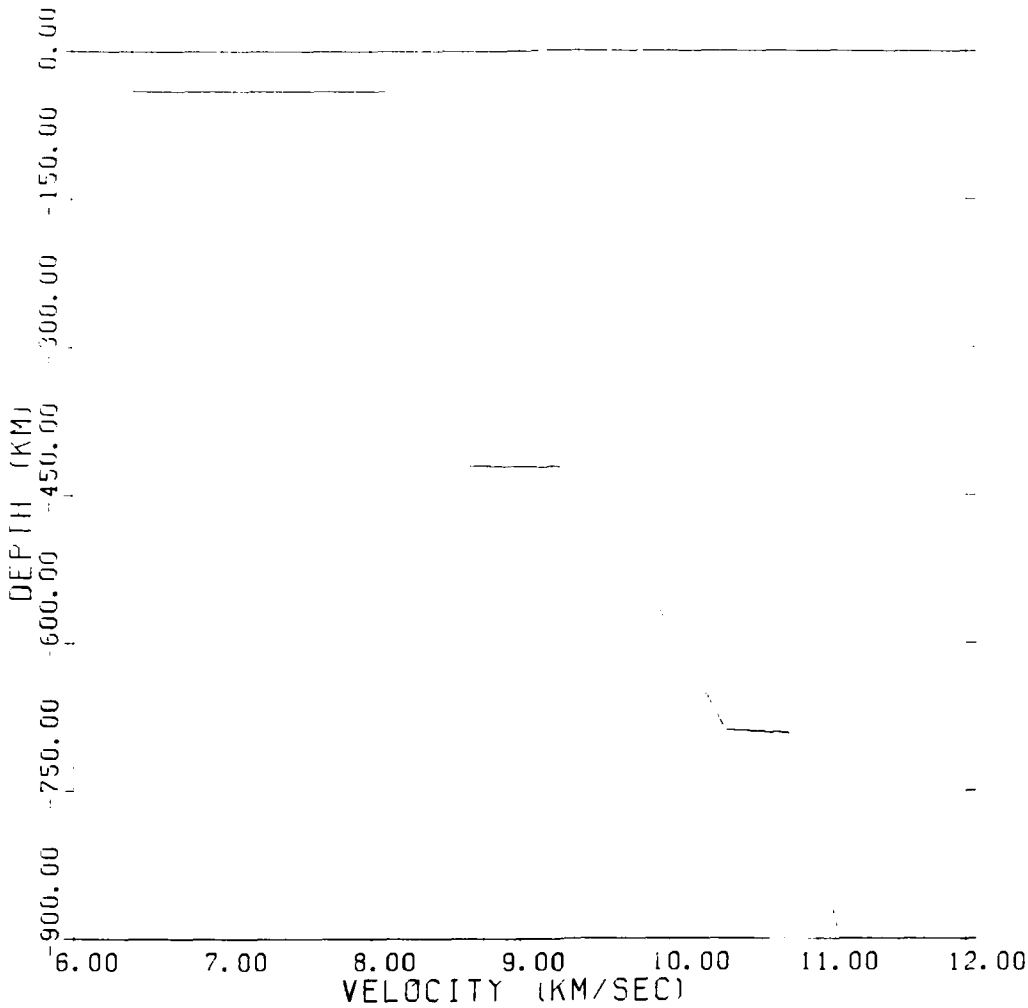

Figure 2. Upper mantle velocity model KCA.

KCA velocity model, and Figure 3 shows a synthetic seismogram record section for the model between 1500 and 3500 km. The synthetics were calculated using a WKBJ method (Chapman, 1976) and include a short period instrument, similar to the ones employed at NORESS, and a constant t* (T/Q) of 0.2 s. Figure 4 shows an example of the available data from explosions at upper mantle distances in northern Europe and western Asia. The source - receiver distribution is shown in Figure 5.

Figure 4 shows that, with few exceptions, the dominant P-wave arrivals are consistent with those predicted by model KCA. However, there is considerable additional complexity that is not predicted by the upper mantle structure. However, we should expect the P-wave coda to be enhanced at these distances, relative to the direct P waves. There will be a coda associated with each of direct P arrivals that will interfere constructively, increasing the overall coda amplitude. On the other hand, the individual P arrivals will not, in general, arrive simultaneously and interfere constructively. Array processing, such as beamforming, stacking, and polarization filtering will clean up these seismograms by reducing near receiver noise, however the signal to noise ratio of the later arrivals will always be higher than at teleseismic ($>30^{o}$) distances. In the following, we will summarize the general behavior of the upper mantle arrivals with attention toward determining those branches that are reliable and easily observed.

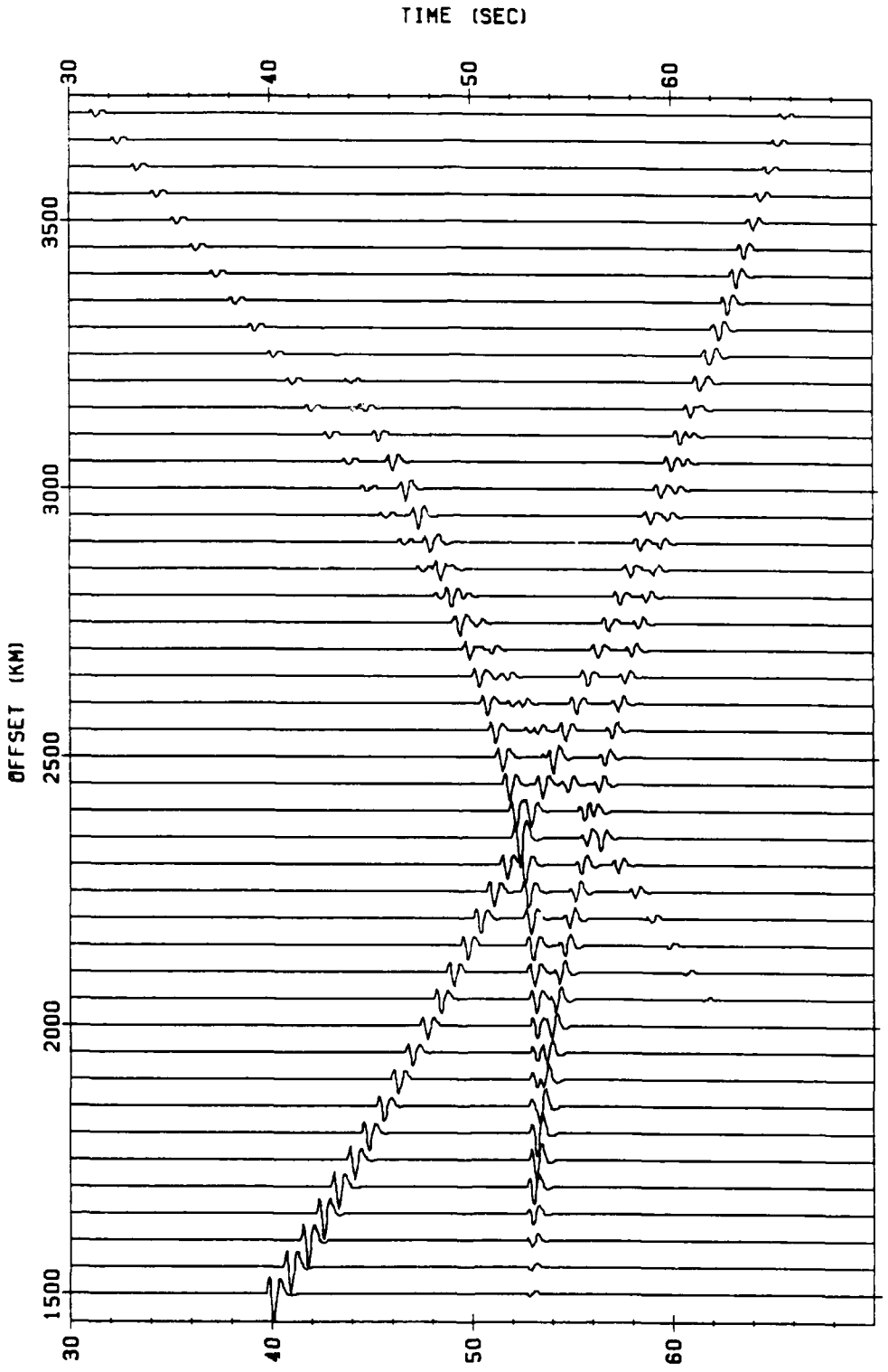

Figure 3. Synthetic seismogram profile for model KCA.

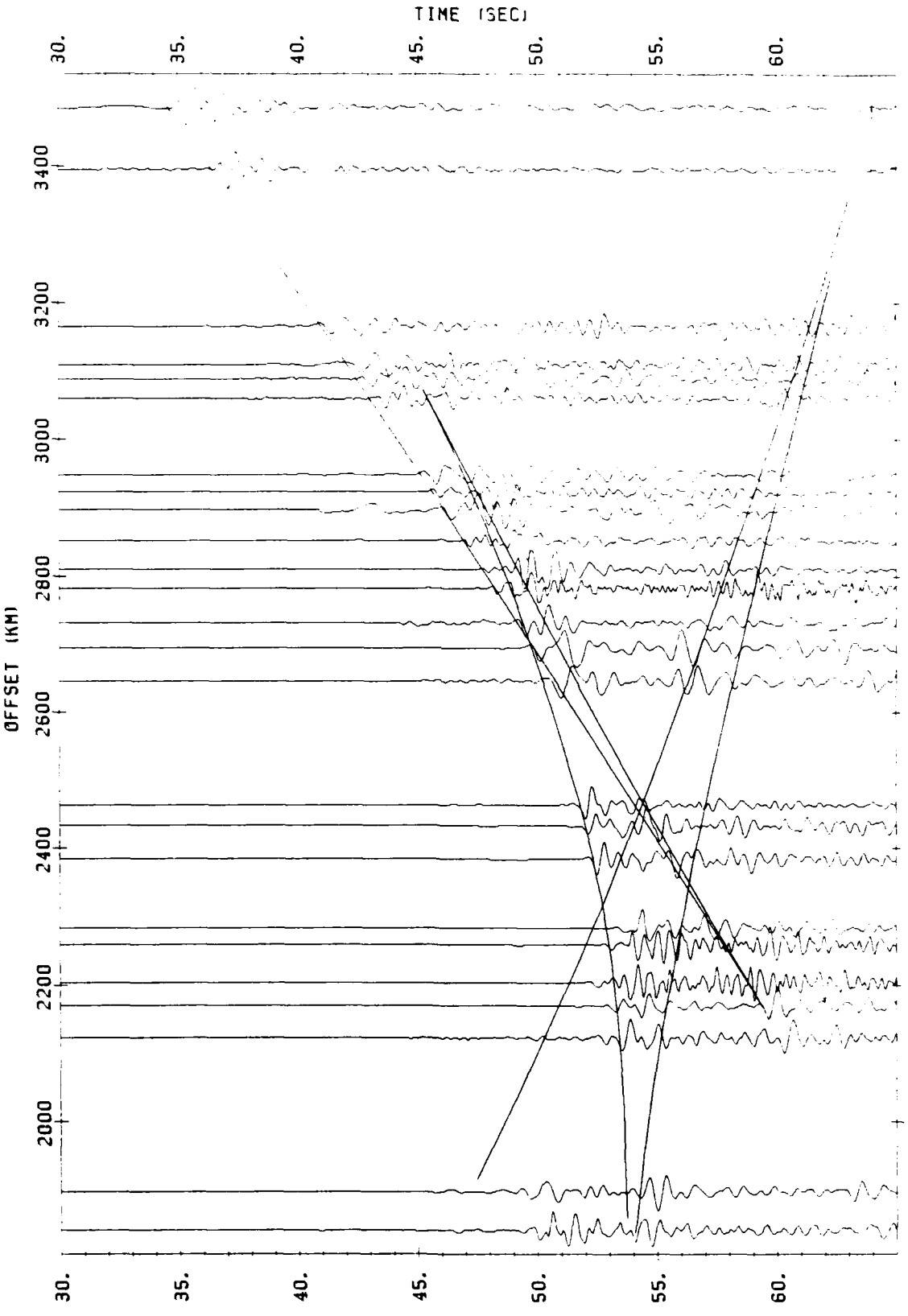

Figure 4. Sample of explosion data from Soviet tests and PNE's.

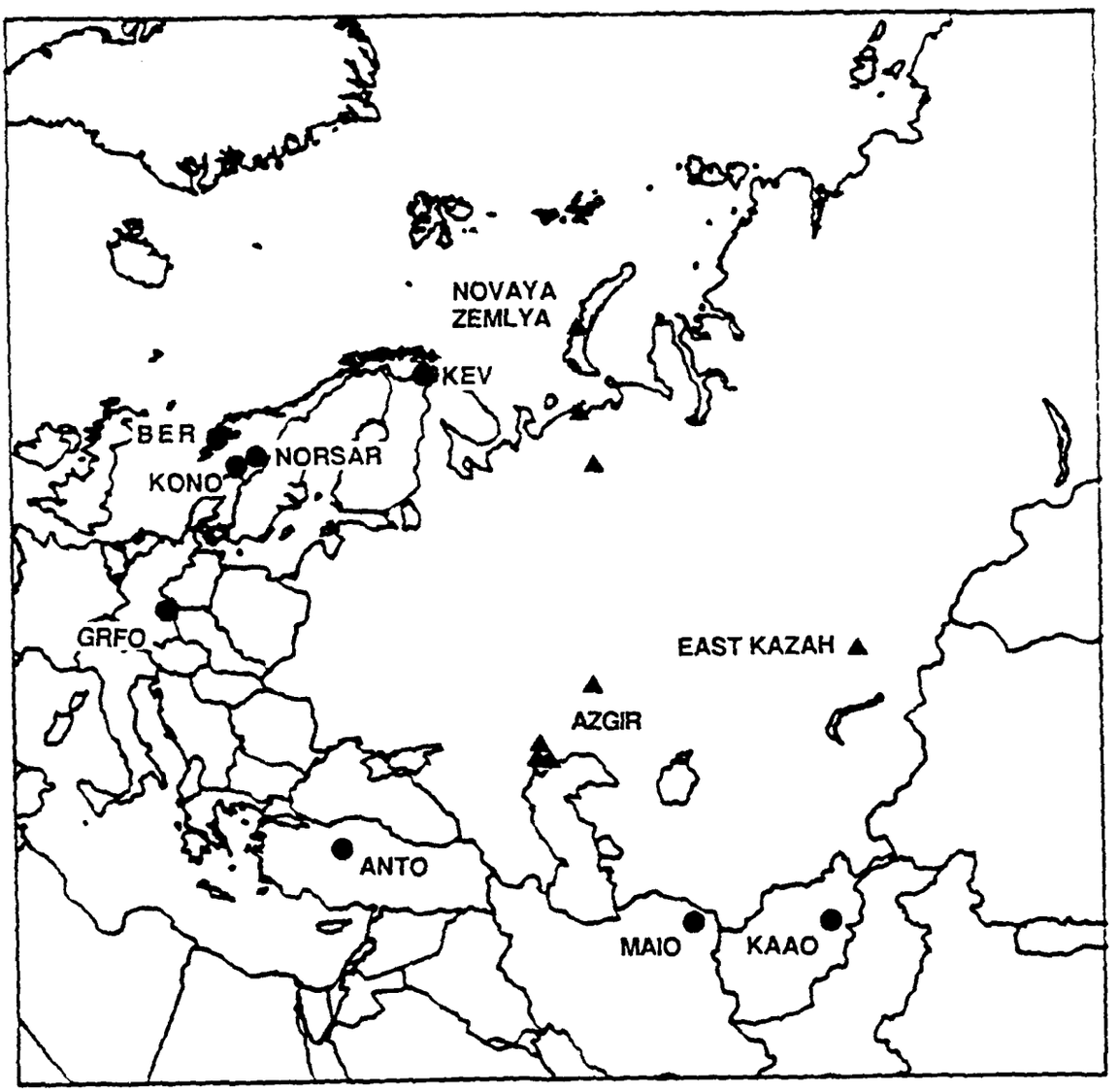

Figure 5. Location map showing station and event distribution for data discussed in this study.

The P_{AB} branch is observed as a strong, discrete arrival between 700 and 1300 km and probably shows little change in character at nearer distances where it is indistinguishable from P_n. Model KCA shows a smoothly varying structure from 40 to 400 km, but little data was available to constrain the upper 150 km. The important feature of the model is the small, positive velocity gradient in that region, which tends to enhance the amplitude of the initial P- arrival. As Figure 4 shows, beyond 1500 km the P_{AB} phase rapidly diminishes in amplitude, relative to the coda, which includes the P_{CD} branch. Thus, the character of the first arrivals becomes more emergent, with observations of very small precursors to the P wave for some source - receiver pairs, such as Novaya Zemlya explosions recorded at NORSAR and NORESS. The P_{AB} branch again appears as a distinct later phase beyond 2500 km, where it becomes sufficiently separated in time from the other, earlier branches. Beyond 2800 km, the P_{AB} phase again becomes an emergent phase with an extended coda. The observability of the P_{AB} phase becomes more erratic and unreliable at larger distances, with occasional observations to ranges of 3800 km. The variability of this phase at distances beyond 2500 km makes it difficult to predict its amplitude; however the arrival time is accurately predicted by model KCA when the phase appears.

In northern Europe and the western Soviet Union, the P_{CD} branch is the dominant arrival in the distance range 1500 to 3000 km. It emerges as a discrete phase 10 to 12 s after the first arrival at 1500 km and

disappears about 4 s after the first arrival at 3000 km. Since the energy travels mostly in the 400 to 700 km depth range, it is less affected by lateral heterogeneity than the energy that travels at shallower depths and thus may be more useful for location purposes and for isolating depth phases. The amplitude of this phase can be as much as a factor of 10 larger than the first arrivals at nearer distance ranges. This enhancement may be due in part to some kind of shadowing of the first arrivals by either attenuation or structure at shallower depths.

At distances between 1700 and 2100 km, there is evidence for a strong phase between the first arrival, P_{AB}, and the P_{CD} arrival. This may suggest additional structure in the upper mantle; however, for our purposes it increases the complexity of the observations and decreases the reliability of identification of the P_{CD} branch.

The P_{EF} phase emerges at 2000 km, delayed about 8 s from the first arrivals and extends to teleseismic distances, becoming the first arrival near 2800 km. The amplitude of this phase is small (by about a factor of 3) relative to the amplitude of the P_{CD} phase, due to the small velocity gradients below the 700 km discontinuity. Therefore, this phase is poorly observed at the nearer ranges where it is a later arrival. In some regions of the world, it is well observed at distances less than 2000 km (e.g. Walck, 1984), which may explain the large later phases on seismograms near 2000 km in Figure 4. These records are from station MAIO for Soviet explosions at East Kazakh,

which is removed from northwest Eurasia but displays many features in the P wave that are similar to those observed in that region.

3.1 Theoretical P Wave Seismograms From 500 to 5000 km for Northwest Eurasia

The synthetic section presented in Figure 3 provides valuable insight into interference and focusing effects due to the velocity structure. However, the computational model ignores some important propagation effects, such as multiple reflections and diffractions, that contribute to the observed complexity in the seismograms. Especially important are the diffraction and reflections that occur off the ends of the triplication branches. To investigate the implications of velocity and attenuation models for using the upper mantle data in source modeling, and to see how well current models predict the observations, we computed a synthetic seismogram section for the distance range 500 to 4000 km. The computational method was a wavenumber integration algorithm (Apsel and Luco, 1984), that computes the complete seismogram, including all multiples, and includes a general, frequency dependent, attenuation model. The P-wave velocity model was a layered approximation to model KCA, the S velocity model was taken from model EU2 of Lerner - Lam and Jordan (1984), and the Q model was adapted from Der et al. (1986); the models are shown in Figure 6. The calculations were carried out to 3 Hz and convolved with a 1 Hz Ricker wavelet (essentially a bandpass filter centered at 1 Hz) for display. The resulting sections for the P-waves are shown in Figure 7a - 7d.

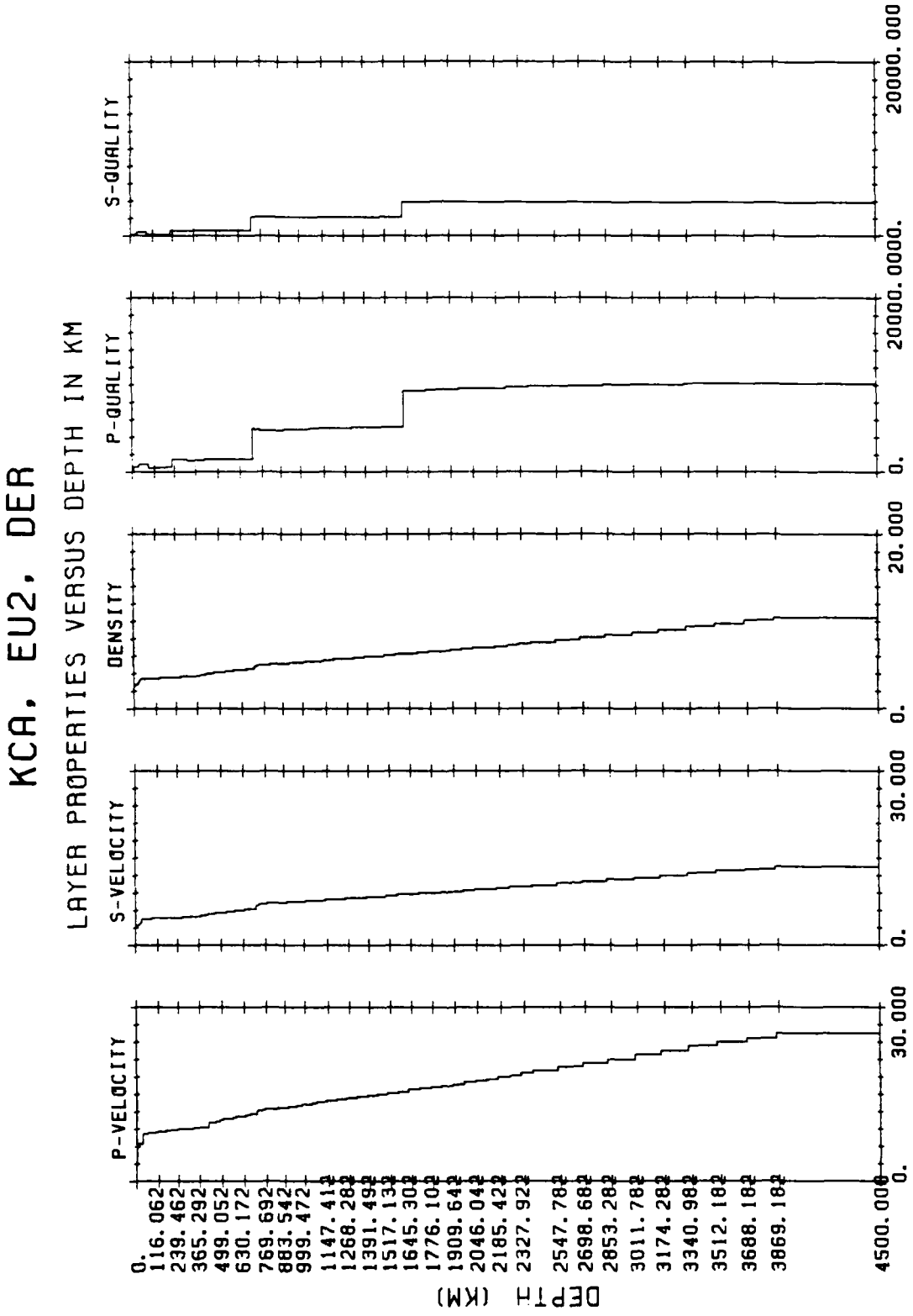

Figure 6a. The velocity, density, and attenuation models used in the theoretical calculations of upper-mantle P and S wave seismograms.

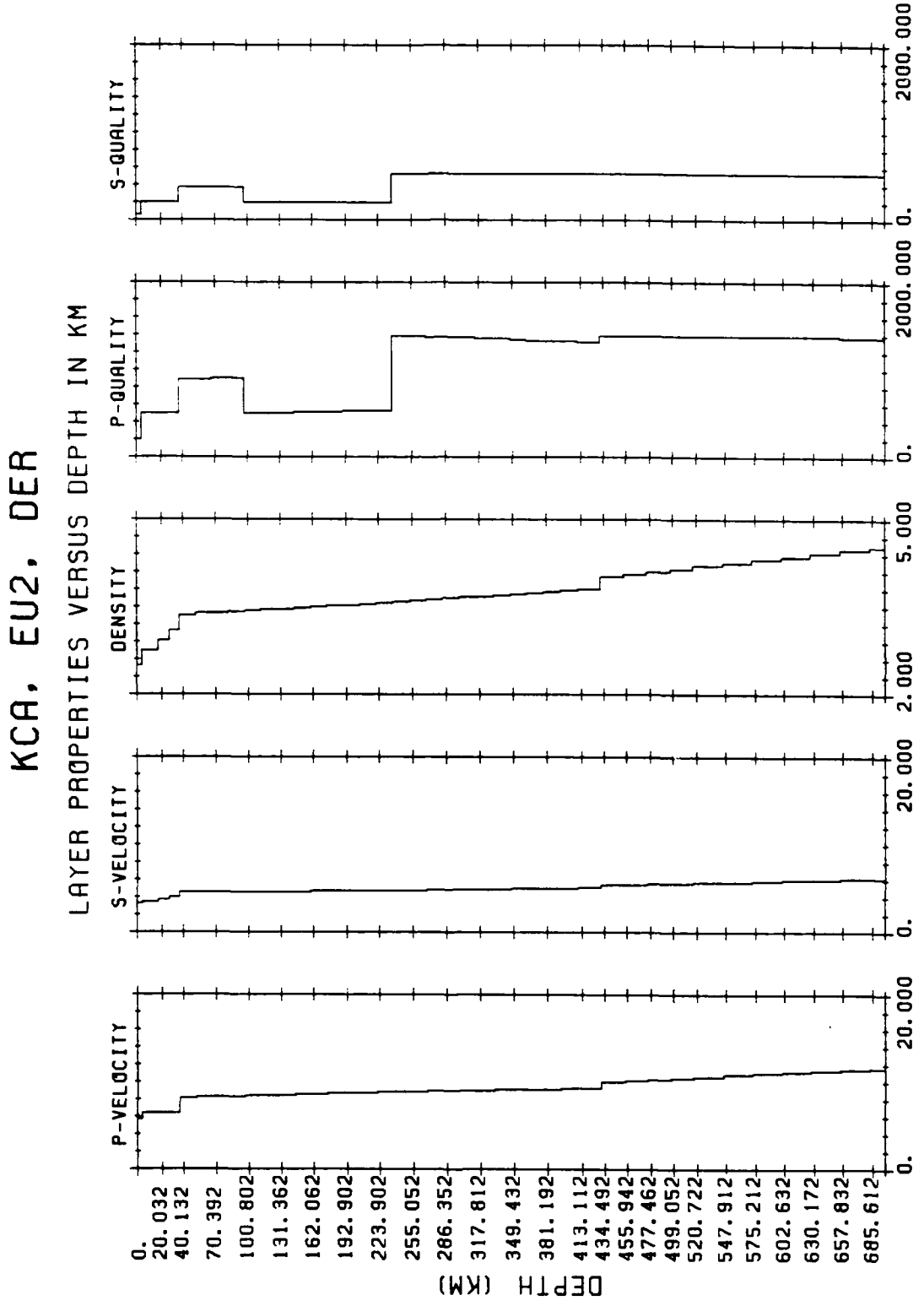

Figure 6b. An expanded view of the upper mantle structure used in the theoretical calculations.

Figure 7a shows a strong P_{AB} (or P_n) between 500 and 1500 km, with the amplitude of the P_n actually increasing between 500 and 1200 km. The reflection from the 400 km discontinuity, the beginning of the P_{CD} phase, should be clearly observable by 1500 km. The P_g (or PmP, the post-critical reflection from the Moho) should be well observed to beyond 1000 km. Langston, (1982) has done similar calculations to model the differences in the P_n and P_g propagation between the eastern and western U. S. His results are similar to ours except that PmP and P_g are separate, due to a midcrustal increase in velocity in his model; thus, the large reflection from the Moho is not as pronounced in his calculations.

The results shown in Figure 7 do not quite predict the observed amplitude decay of the P_{AB} branch beyond 1300 km. Typical examples of the amplitude decay are shown in Figures 8 and 9. Figure 9 is taken from Given (1984) and is consistent with the data presented in King and Calcagnile (1976) for this distance range (see their Figure 2). The misfit in relative amplitudes can easily be explained by an increase in attenuation in the uppermost mantle. Otherwise, the models of velocity and attenuation qualitatively predict the observed seismograms from northwest Eurasia.

Several features of the calculations are particularly worth noting. The peak amplitude between 800 and 3000 km is virtually constant and a factor of 3 or so larger than the amplitudes predicted for teleseismic

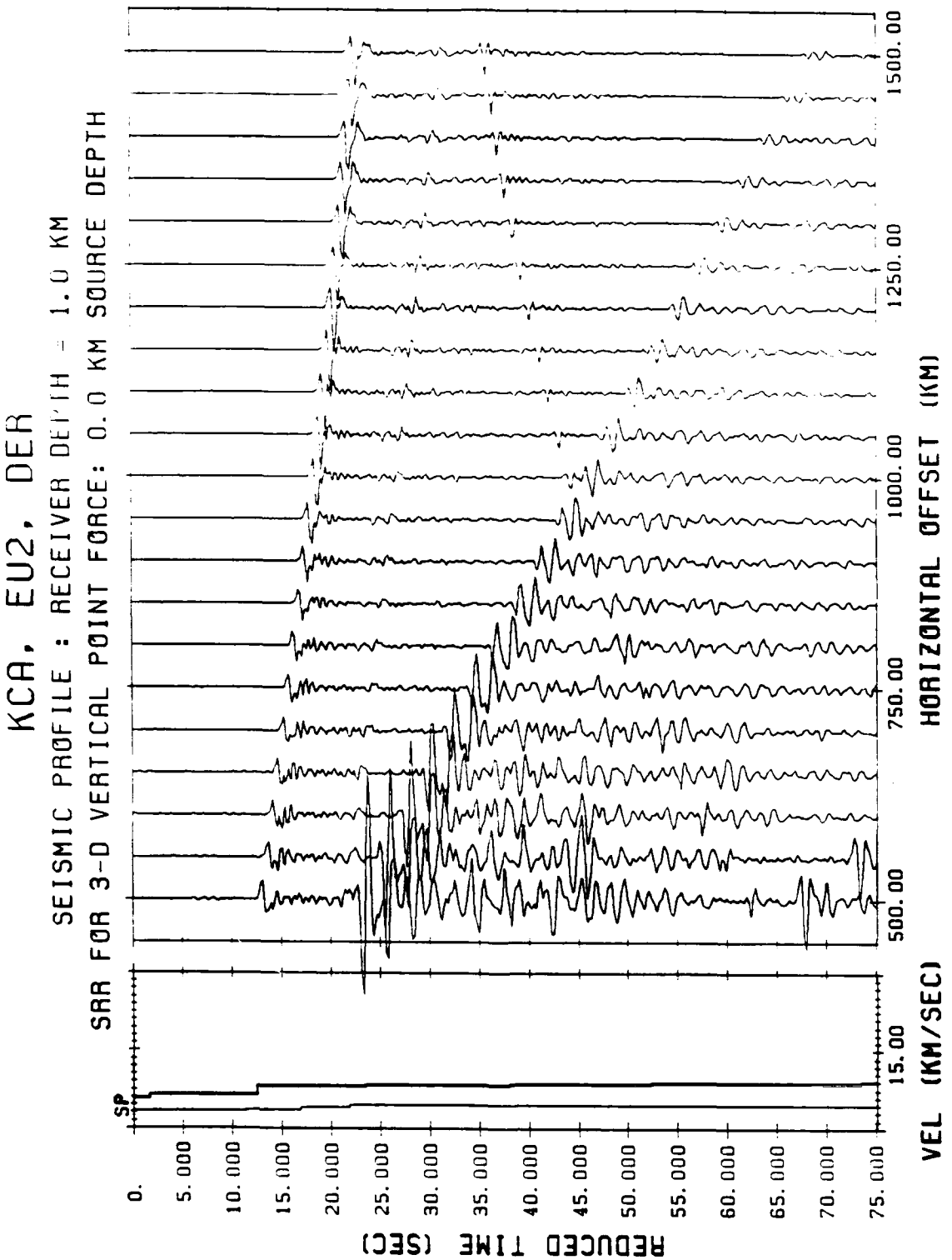

Figure 7a. Vertical component theoretical seismograms from an explosion source at 1 km depth recorded at distances from 500 to 1500 km.

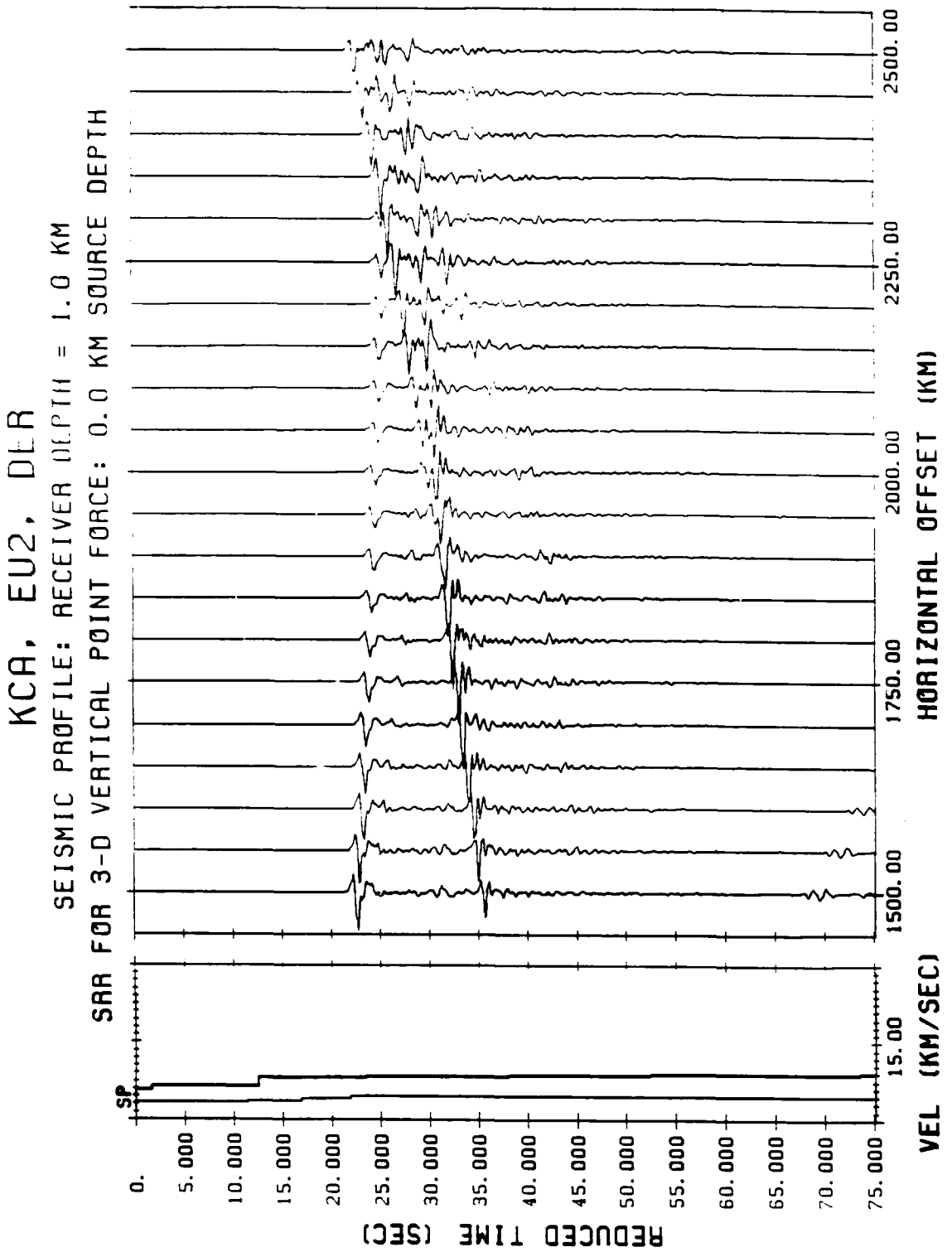

Figure 7b. Seismograms calculated at distances between 1500 and 2500 km.

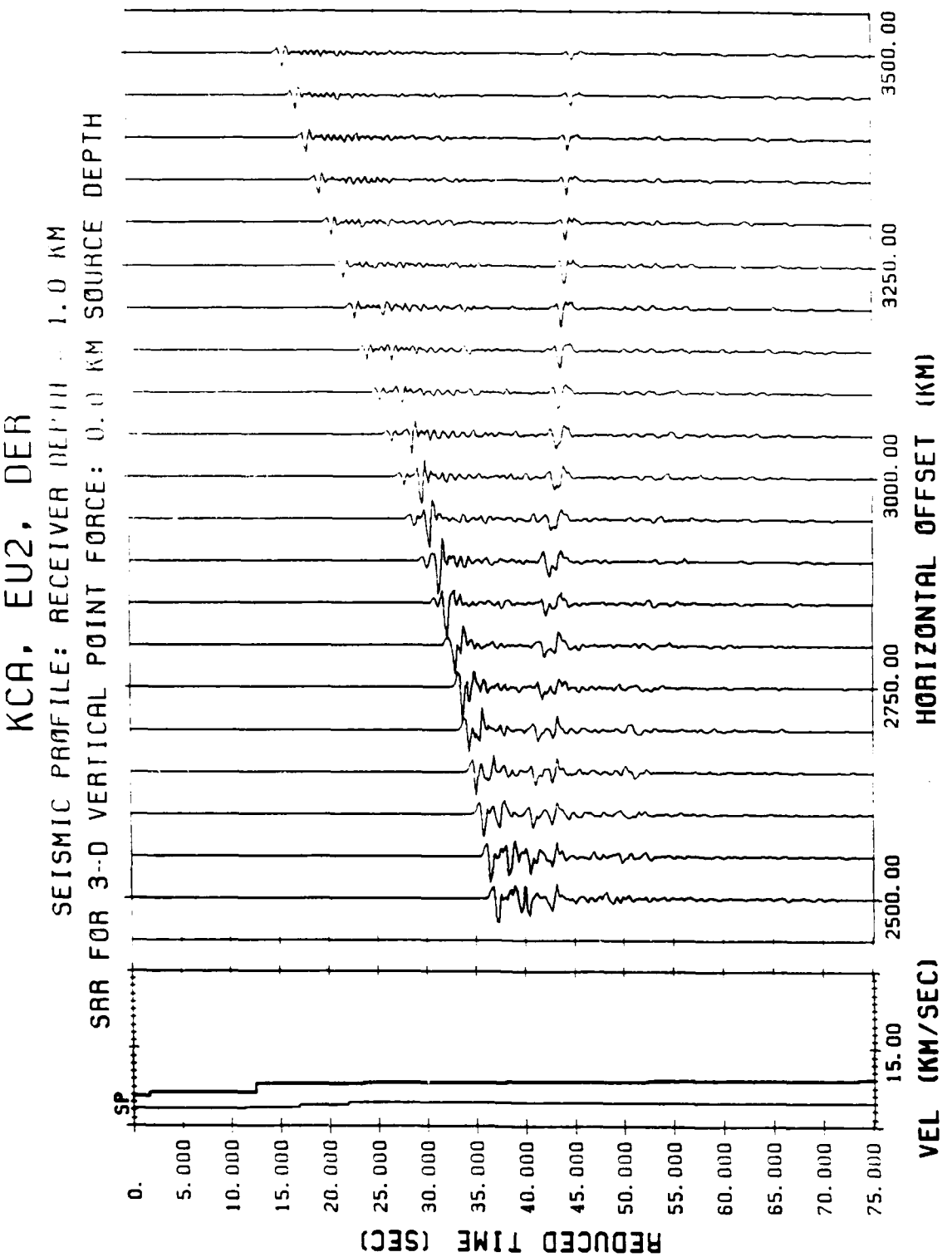

Figure 7c. Seismograms calculated at distances between 2500 and 3500 km.

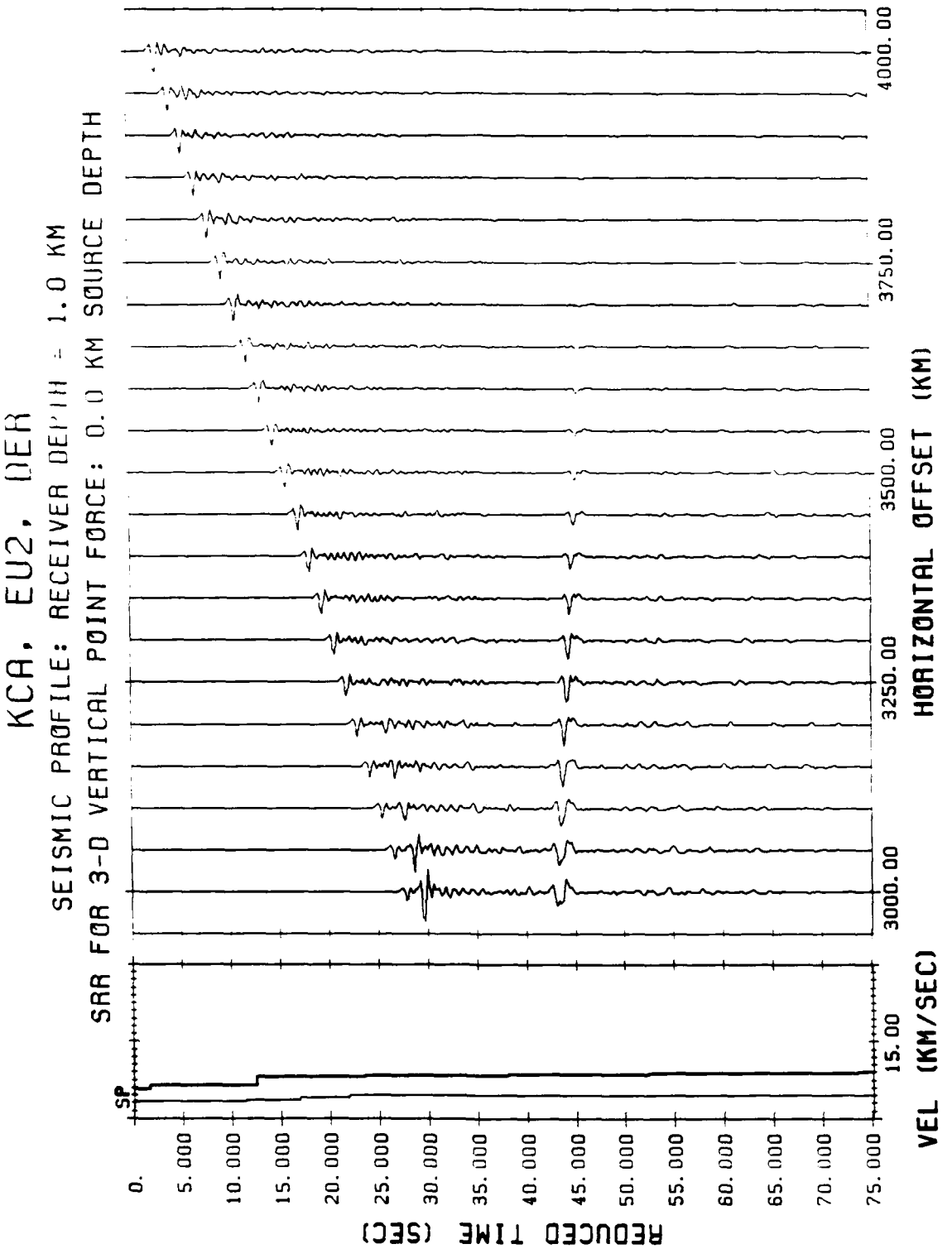

Figure 7d. Seismograms calculated at distances between 3000 and 4000 km.

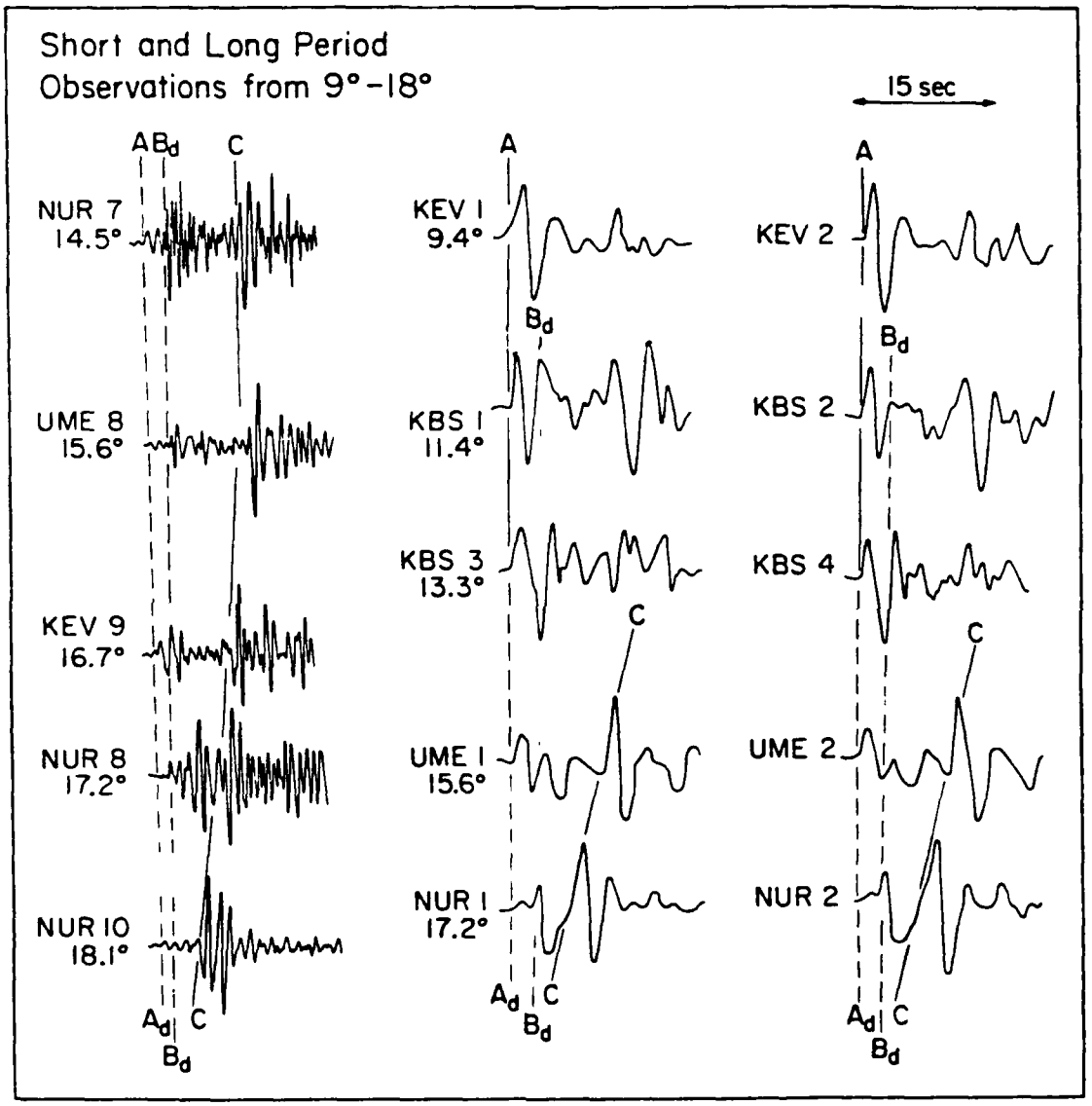

Figure 8. Observed seismograms of Soviet presumed explosions recorded on short and long period WWSSN seismograms.

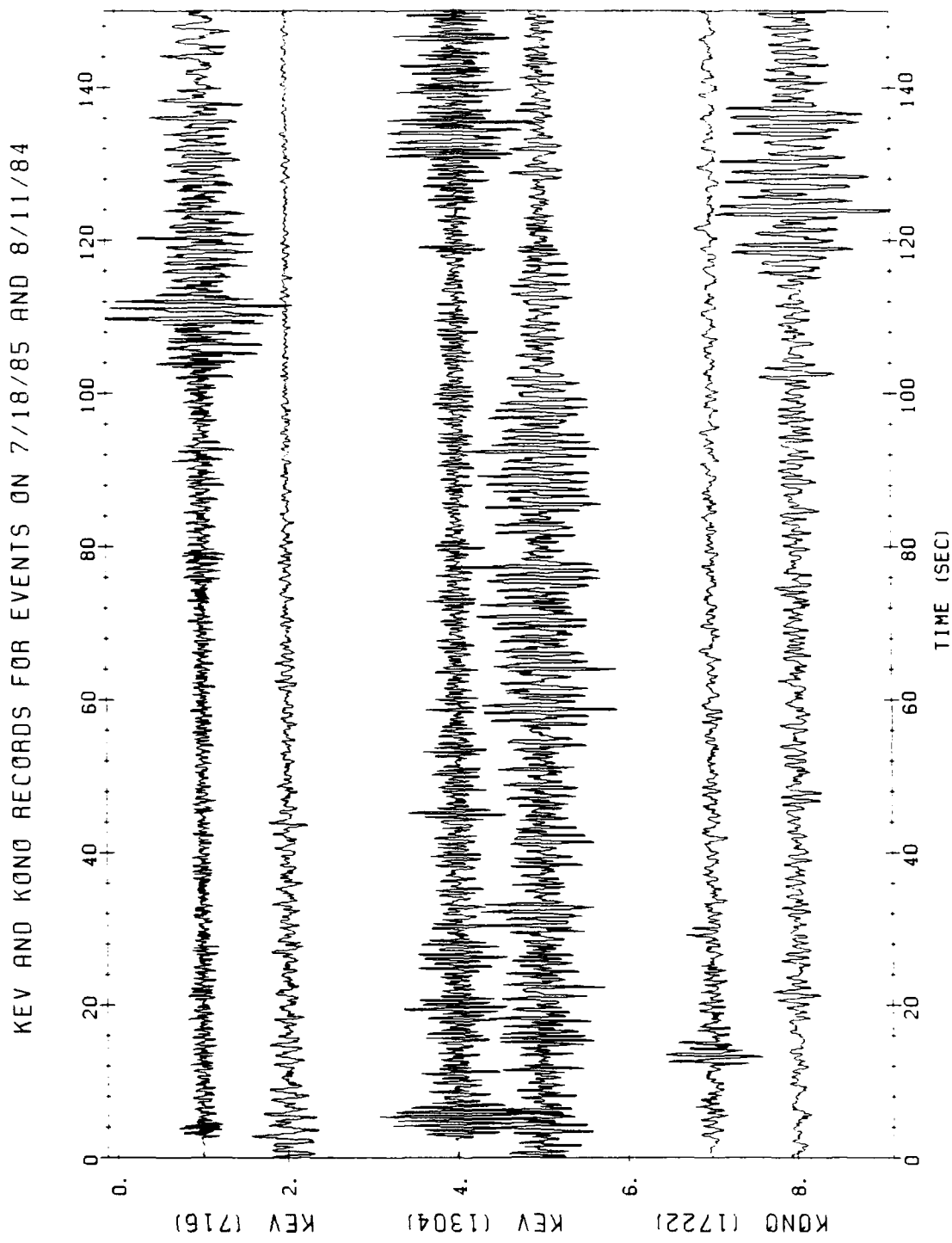

Figure 9. Observed seismograms from Soviet PNE's showing character of P_{AB} between 700 and 1800 km.

distances. Thus, there appears further reason to suspect that there will be significant signal enhancement at these ranges. The retrograde travel time branches, P_{BC} and P_{DE}, are predicted to be of significant amplitude and, when all 5 branches are arriving at distances between 2000 and 2500 km, the seismograms are very complex for nearly 10 seconds. It will be very difficult to use data at these distances for detailed source determination.

We note further that these models predict simple, impulsive, P_n and S_n phases from 700 to 1500 km that should be well observed and very sensitive to the source mechanism. Since S wave radiation should be a powerful discriminant, it is useful to present some observations that support these models at distances between 700 and 1500 km. Figures 10 and 11 show two Novaya Zemlya explosions recorded at the digital WWSSN station at KEV, Finland. P_n does show some unexpected complexity; in particular, there is a large second phase delayed by 12 s that is not predicted by the theoretical calculations. This may be due to a high velocity layer in the lower crust, or it may be a PP phase. A small PP phase is seen about 9 sec after the initial P in the synthetic section in Figure 7a. S_n also appears particularly strong in Figures 10 and 11, indicating significant S wave radiation for these events. Figures 12 and 13 show the same seismograms after a high pass filter with a corner at 4 Hz has been applied. At the high frequencies, the large amplitude S_n phase has been substantially attenuated.

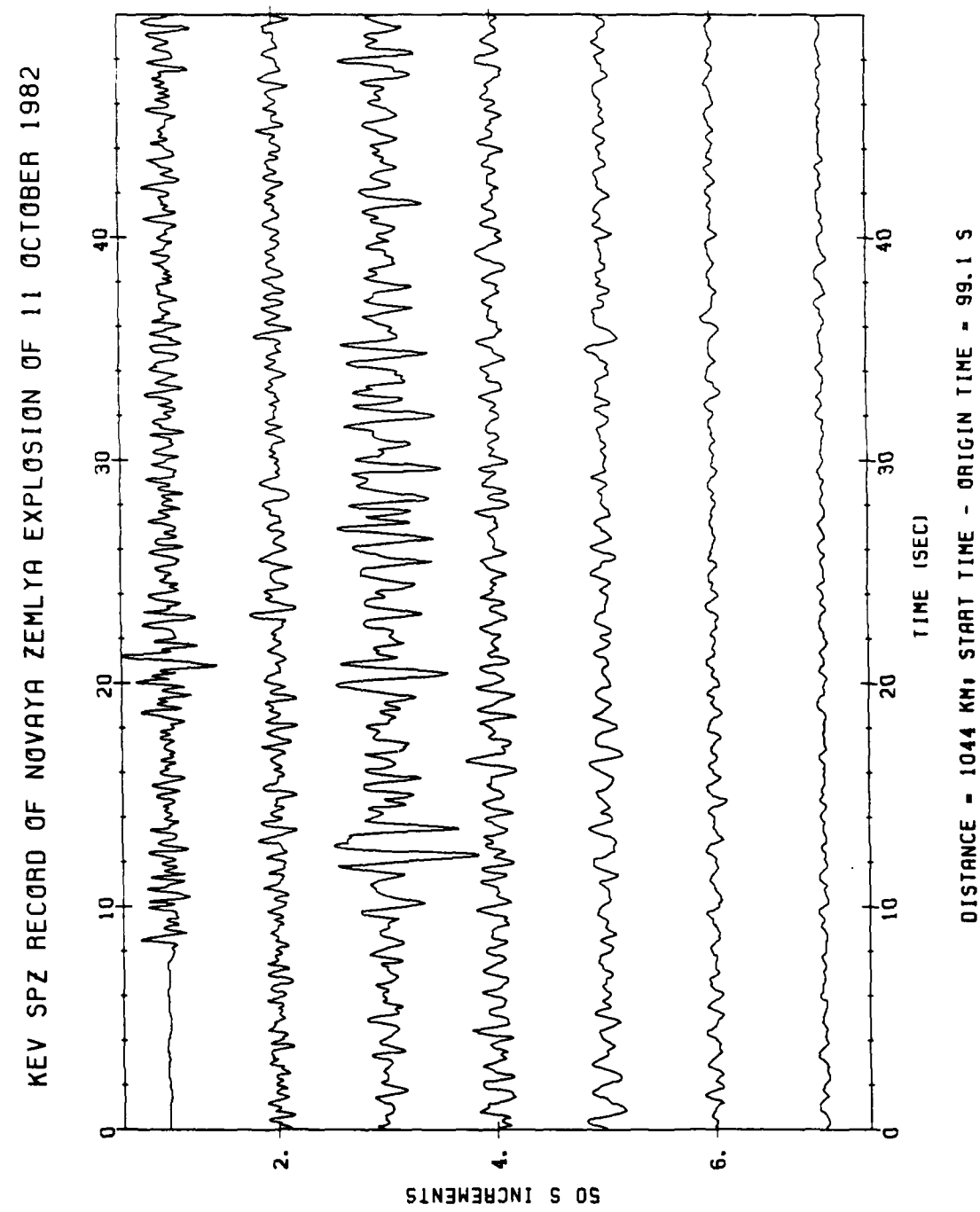

Figure 10. Observed short-period vertical seismograms at DWWSSN station KEV from Novaya Zemlya explosion.

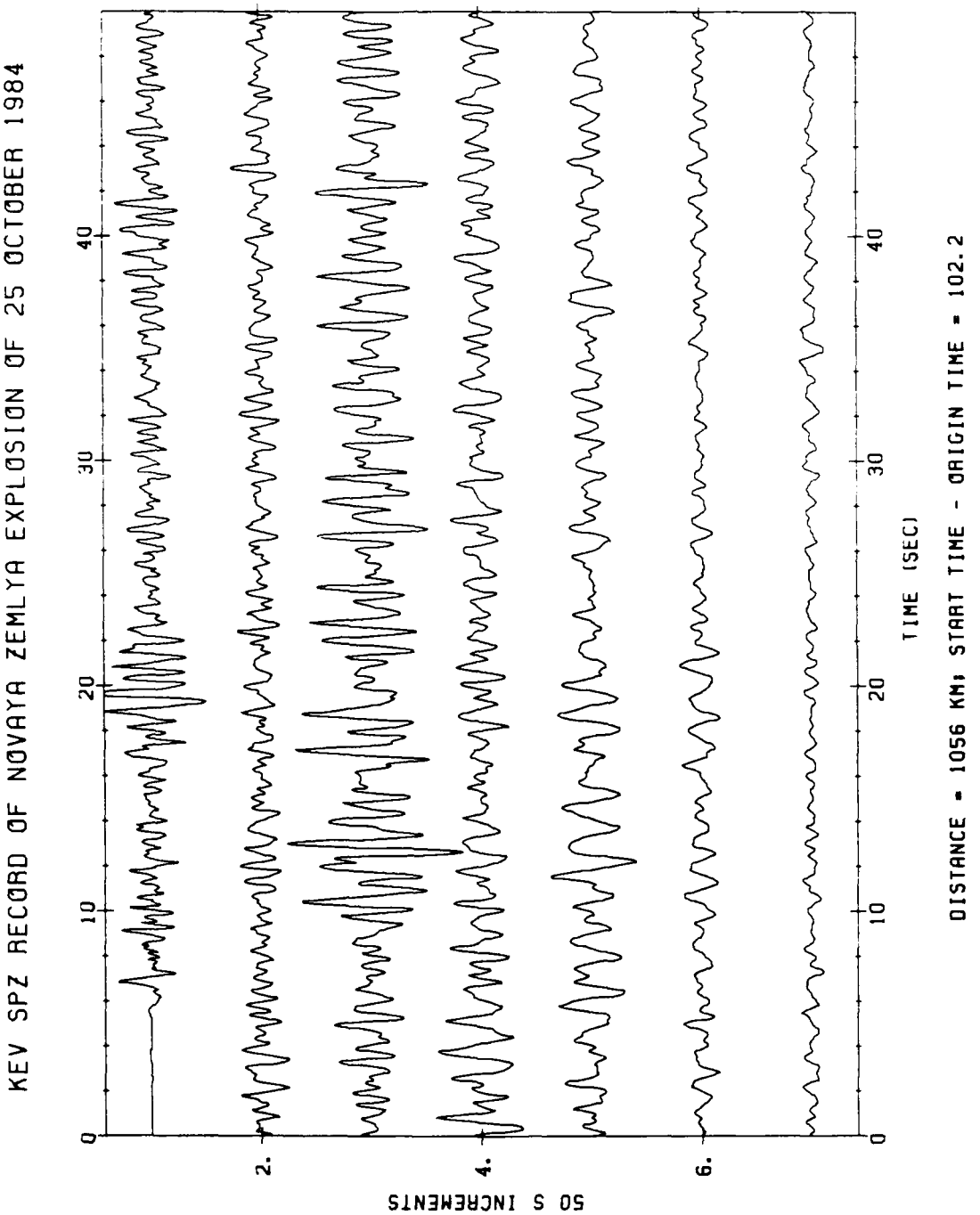

Figure 11. Observed short-period vertical seismograms at DWWSSN station KEV from Novaya Zemlya explosion.

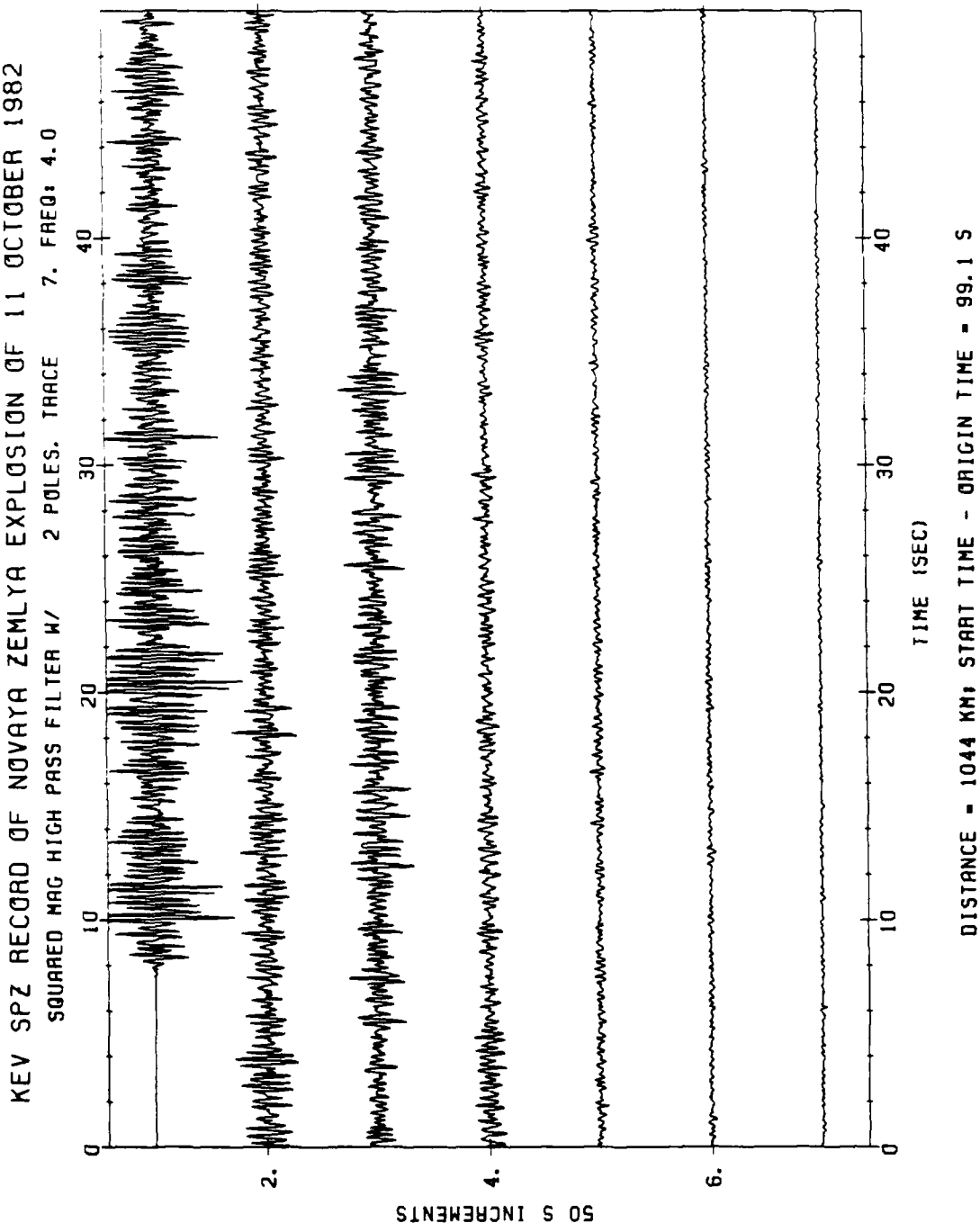

Figure 12. Same seismogram as shown in Figure 10 except filtered with high pass filter at 4Hz.

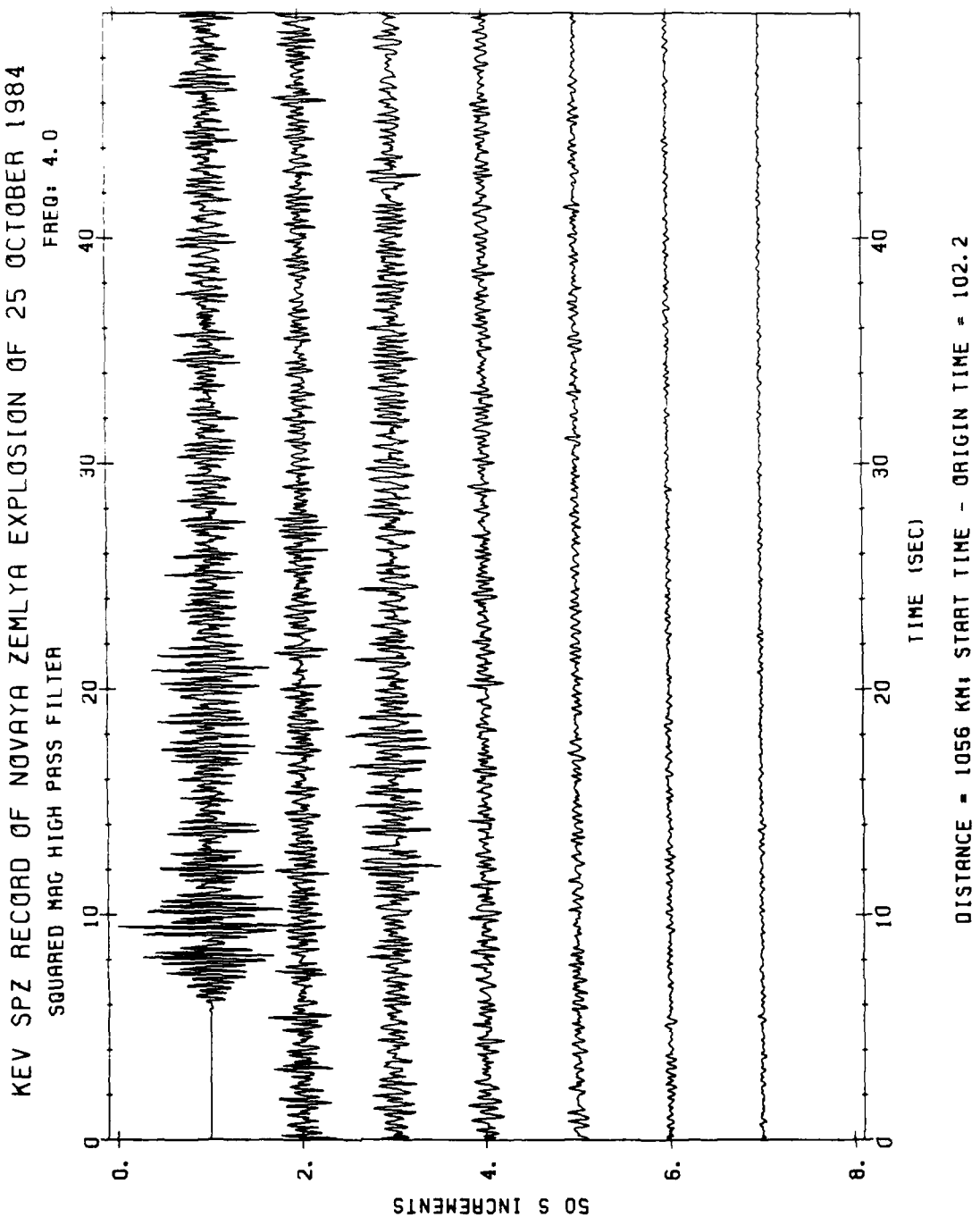

Figure 13. Same seismogram as shown in Figure 11 except filtered with high pass filter at 4 Hz.

These observations are repeated at the same station for other explosions at different distances and azimuths. Figures 14, 15, 16, and 17 show unfiltered and filtered seismograms from two other explosions in Western Russia. At 700 km the S_n phase and P_n phase are roughly the same amplitude and this does not change for the filtered results. For the observation at 1300 km, the P_n phase is, again, enhanced at the higher frequencies relative to S_n. Of course these observations are single component, short period vertical instrument and S_n should be more readily observed on three component instruments. Nevertheless the velocity and attenuation structures predicted for this region imply that both S_n and P_n should be well observed and should be very sensitive to the source mechanism. The biggest problem in utilizing this data is taking into account the large variations in the propagation path, and detecting whether S_n and P_n amplitudes are being affected by propagation anomalies or source radiation.

3.2 Path Calibration Considerations

Calibrating the upper mantle structure of northern Europe and western Russia is a relatively straightforward task. The Soviets have detonated numerous tests at several different sites and have used nuclear explosions for construction projects throughout the region. With the proximity of the NORSAR array, studies like that of King and Calcagnile (1976) enable the determination of the important features

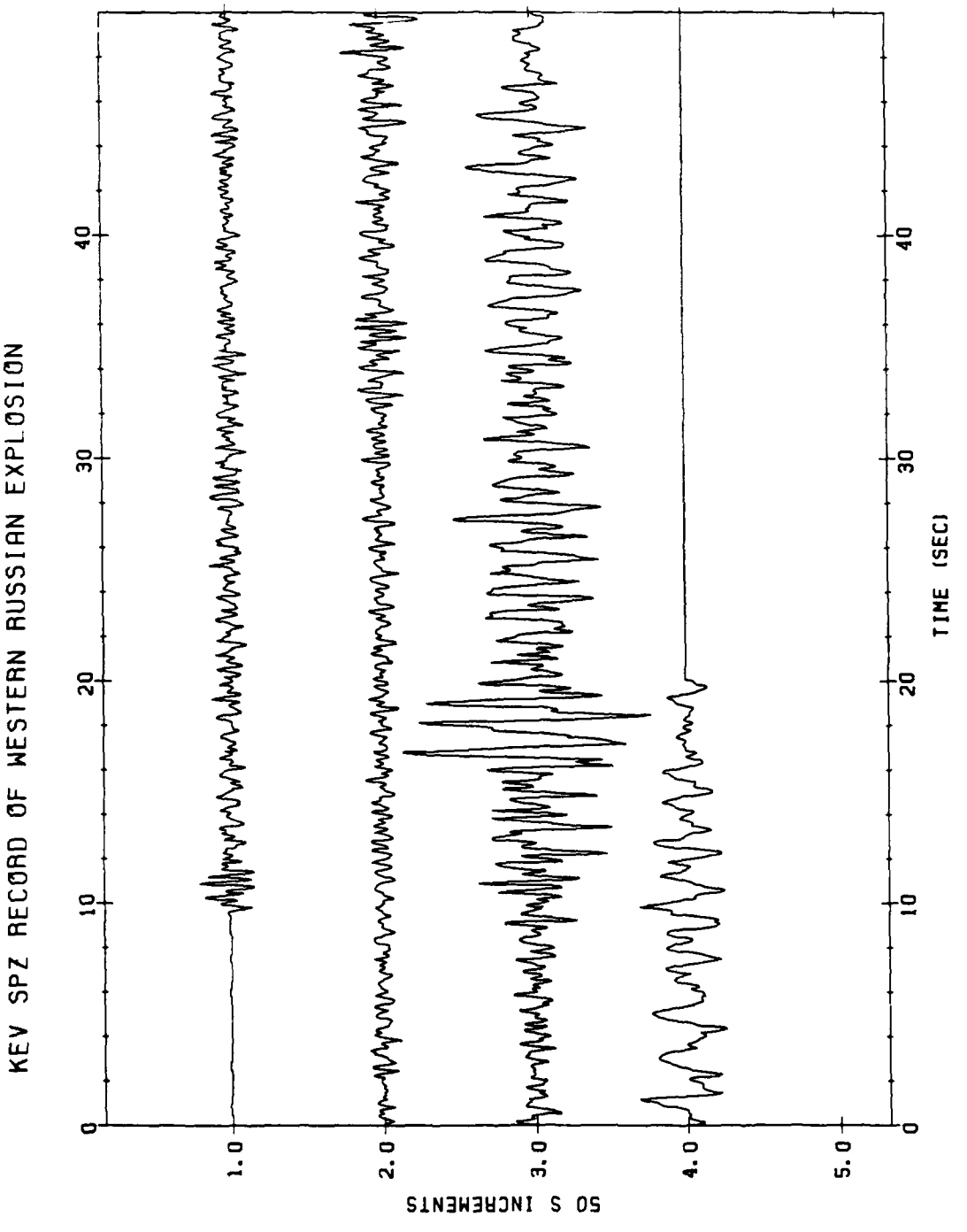

Figure 14. KEV DWWSSN SPZ seismogram of Soviet PNE on 21:14:57, 18 July 1985 at distance of 714 km.

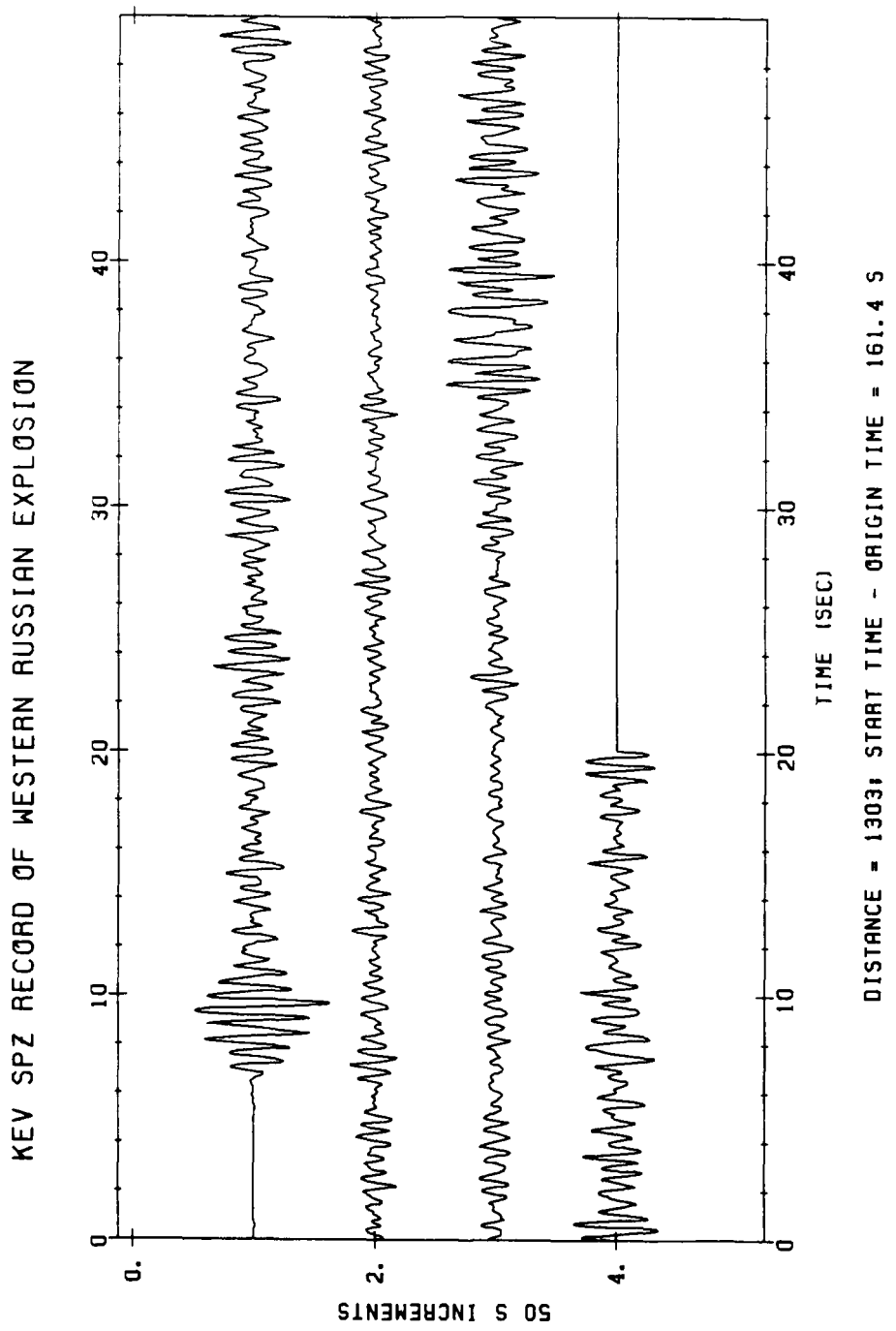

Figure 15. KEV DWWSSN SPZ seismogram of Soviet PNE on 18:59:57, 11 August 1984 at distance of 1304 km.

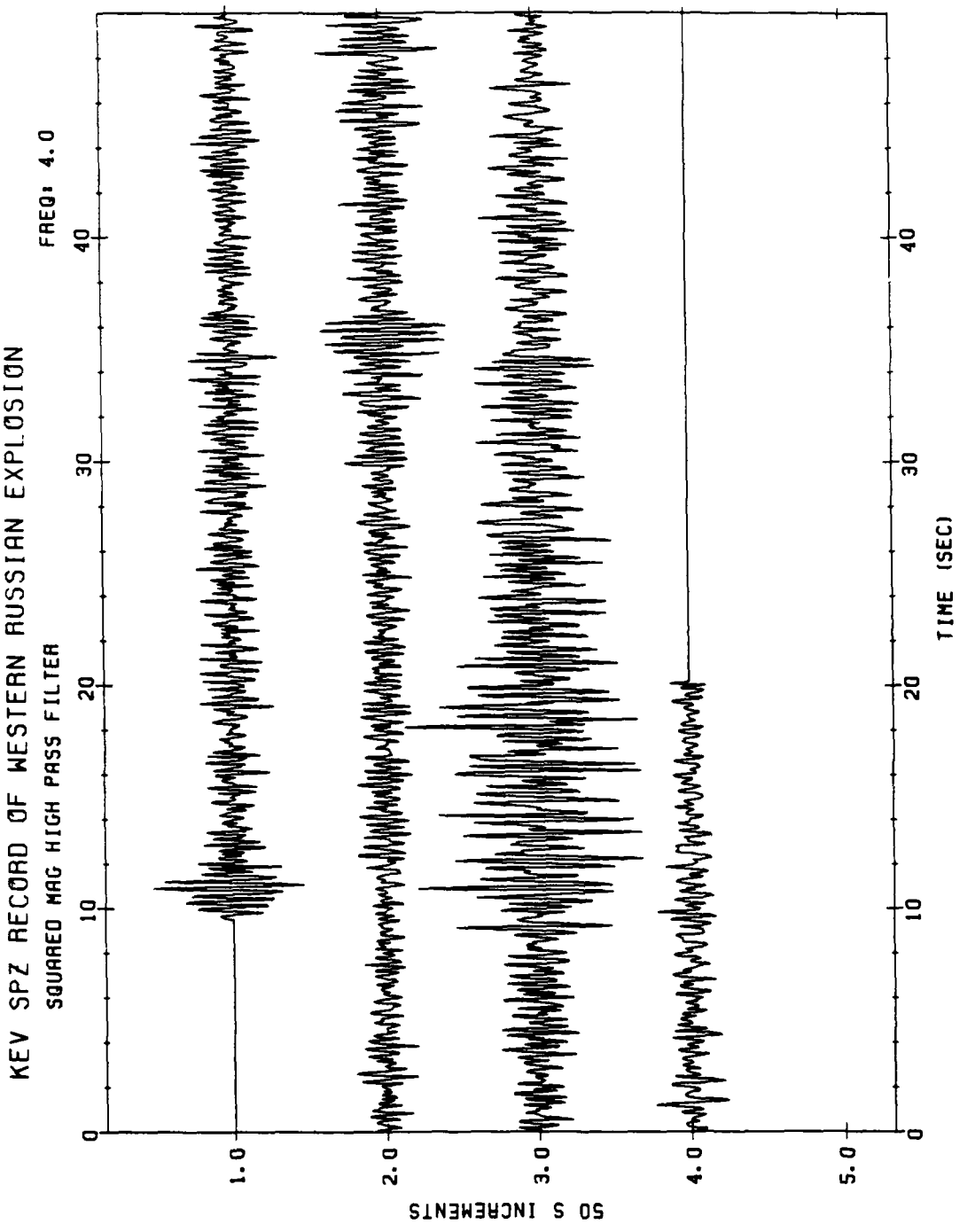

Figure 16. Same seismogram as shown in Figure 14 except high-pass filtered at 4 Hz.

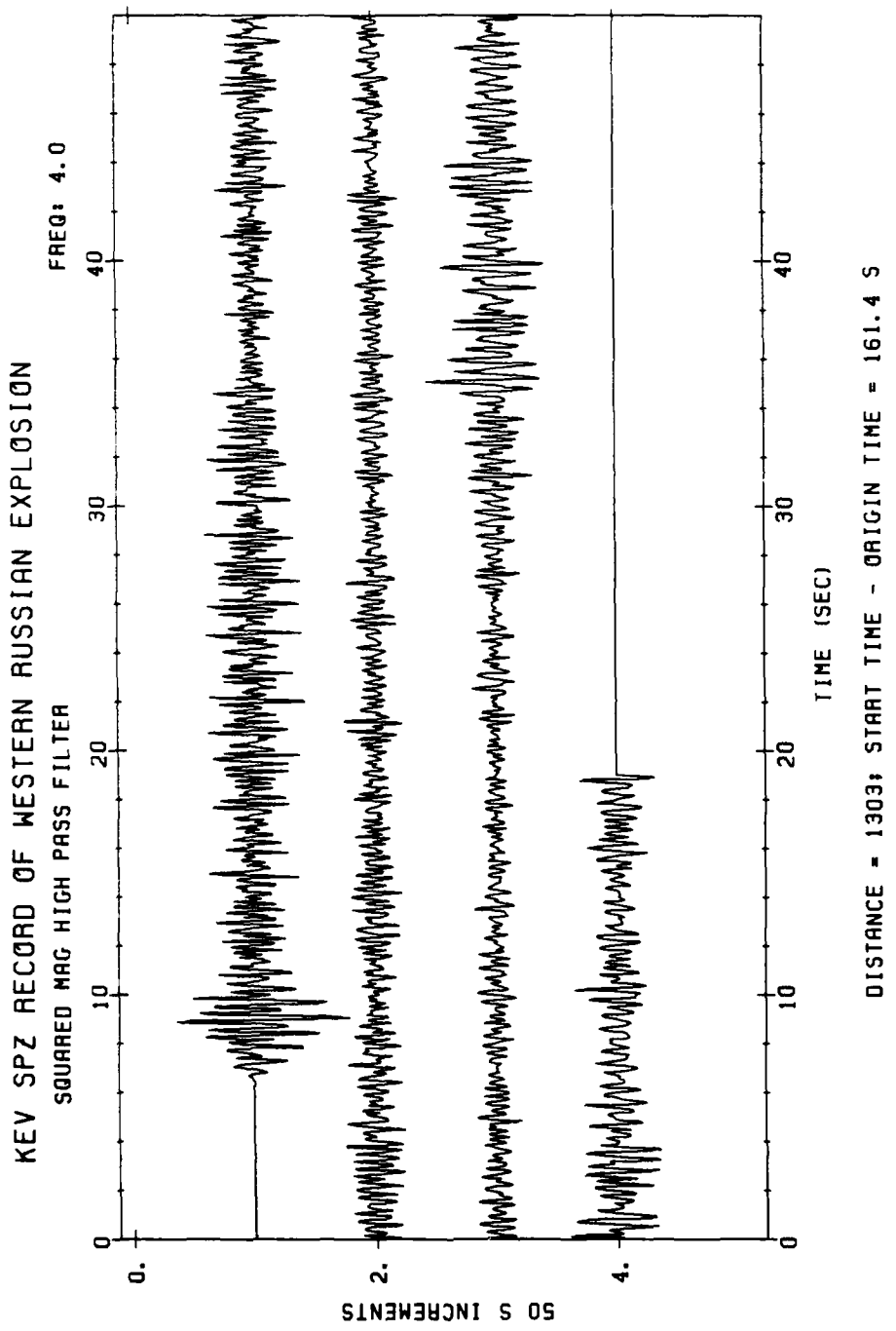

Figure 17. Same seismogram as shown in Figure 15 except high-pass filtered at 4 Hz.

of the velocity structure. The availability of additional data from the GDSN and WWSSN stations in northwest Eurasia helps to confirm the important predictable details of the uppermantle seismograms and indicate the effects of lateral variations in the structure.

A program to monitor small nuclear explosions throughout Asia with a network of seismographs will require that we determine the upper mantle structure in a region where very little data of any kind has been previously available. Lacking the high quality explosion data available from western Russia, we will need to develop ways to use earthquake seismograms to estimate the effects of structure on the seismograms. Arrays and networks have found widespread use for determining upper mantle structure using data from earthquakes, (e.g. Simpson, et al., 1974; Walck, 1984, 1985). Studies using earthquake data recorded at NORSAR and UKAE arrays have had some success in estimating the velocity structure (e.g. England et al., 1977), however the arrays necessary to determine the velocity structure in central and eastern Asia may not be available. Therefore, we need to develop the capability to use earthquake seismograms to constrain the important features of the P waves at upper mantle distances.

In contrast to previous scientific studies, in which the velocity structure was the objective and precise measurement of travel time and apparent velocities were emphasized, our desired regionalization requires only that we recognize the presence of later arriving branches and their approximate arrival times. While measuring the arrival times of the different branches to an accuracy of 0.5-1.0 s is

not sufficient for detailed velocity analysis, it may be adequate for our purpose of recognizing the major upper mantle arrivals. Thus it may be possible to use earthquake seismograms from individual stations, which have been processed to minimize the effects of local receiver structure, to estimate what an explosion should look like in regions where no explosion data is available.

A substantial effort was directed toward developing techniques to isolate upper mantle branches in earthquake data using the NORESS array. High quality array data, or 3 - component data, was deemed necessary to minimize contamination due to near receiver structure. It was hoped that sufficient data could be obtained to implement a velocity stacking method to define "average" seismograms for a given region. Clearly, a large amount of data would be required to account for the tremendous variation in earthquake seismograms due to radiation patterns, depth effects, and complex sources.

Our approach to processing the data is similar to those methods used to interpolate seismic reflection and refraction data in the tau - p, or intercept time - apparent velocity, domain (Thorson and Claerbout, 1985; Kappus et al., 1987). Transformation from the time - distance domain to the tau - p domain is accomplished via a generalized inverse algorithm in order to account for missing and erratic data. To account for unknown polarities, the envelopes of the seismograms can be used. The result of the processing is a tau - p representation of the seismic wavefield, valid over the range of distances spanned by the input data, that can be inverted to determine a representative

seismogram at any distance within that range. This representative seismogram will show the effects of the upper mantle structure including relative amplitudes of the major branches; the complexities due to depth and radiation patterns are attenuated, since they should vary randomly between seismograms.

Unfortunately, this part of the study required substantially more resources than was originally anticipated, and at the time, the necessary data was not available. The preliminary results showed arrivals that agreed with known structural effects, but the large variations in the earthquake data introduced an unacceptable amount of noise into the interpolated seismograms, suggesting that a large amount of carefully selected data may be necessary. However, in an environment with efficient access to a large database of high-quality seismograms, the approach may prove useful for estimating the structural effects on regional and upper mantle seismograms.

4.0 Evaluation of the Pearce Algorithm at Upper Mantle Distances Using a Complexity Measure

Previous studies have evaluated the Pearce algorithm applied to the analysis of events using teleseismic data (McLaughlin et al., 1983). In our previous report, (Given et al., 1987) we have shown how the algorithm may be applied to events using data from upper mantle distances. To further evaluate the performance of the Pearce algorithm as a discrimination tool, we would prefer to analyze a number of individual events. However, we are interested in small events with high quality short period data from a restricted distance range (5^{o} to 30^{o}) and few small explosions or earthquakes have the necessary coverage with modern instrumentation to adequately constrain, or rule out, a double couple mechanism. Another way to evaluate the potential performance of the Pearce algorithm using data at these distances is to put constraints on the relative amplitudes of possible depth phases based on actual observations of explosions at upper mantle distances. In other words, we will estimate how large a depth phase (pP or sP) can be hidden in the coda of the observed explosion seismograms. Using these constraints, we can then determine what source - receiver geometry is necessary to provide the minimum amount of useful information and what the depth limitations of the method are.

Synthetic tests using the Pearce algorithm have shown that, for simple explosions, P-wave observations at 3 to 5 azimuthally well-distributed

stations at upper mantle distances are sufficient to rule out all possible earthquake focal mechanisms if the reflected phases pP and sP can be constrained to be smaller than that of direct P (Given et al., 1987; McLaughlin et al., 1983). This theoretical result provides a basis for a complexity measurement that can be used to assess the usefulness of a set of seismograms recorded from earthquakes and explosions.

As discussed earlier, the velocity structure of the upper mantle produces triplications in which there are as many as 5 arrivals from a single source at distances between 1500 and 3500 km. Even so, if the arrival times of the triplicated phases can be accurately predicted, the amplitudes of arrivals not associated with the direct P arrivals can be used to constrain the maximum relative amplitudes of the depth phases. Therefore, we must first determine the appropriate regionalization and upper mantle velocity structure necessary to confidently estimate the arrival times of the different branches. In a previous section of this report, and in our previous report, we discussed the features of the observed seismograms at upper- mantle distances in northwest Eurasia. For this part of the world, there has been sufficient calibration to characterize the appearance of ▸, explosion seismograms at upper mantle distances. We will develop and evaluate our complexity model for this region using the conclusions presented in those summaries.

Figure 4 is a section of upper mantle seismograms from explosions in the region with the travel time curve KCA superposed. These data are from a wide region of central and western Asia and northern Europe, yet, the KCA travel time curve accurately predicts the dominant arrivals. Based on the agreement between the predicted and observed phases, we determined time windows in which P-wave arrivals were expected. The amplitude that occurs in these windows is taken to be the amplitude of the direct P; the amplitude of the signal outside the windows is used to estimate the minimum amplitude of observable surface reflections. The windows are shown in Figure 18. Obviously, if the depth phases arrive inside the windows, they cannot be distinguished from the direct P phases and, therefore, there is a limit to the depth resolution of the potential discriminant. The resolvability is summarized in Figure 19 in which the possible depths that can be resolved are plotted versus the distance between station and event. Figure 19 is pessimistic, since if we have some prior experience in an area and know what to expect as dominant phases, we may do much better. An example is the arrival from the 400 km discontinuity (P_{CD}) in northwest Eurasia. It is such a dominant later phase that it alone could be used to estimate amplitudes of possible surface reflections, substantially reducing the unresolvability.

There are many possible ways of defining and measuring complexity. We chose a very simple one that fits with our model of the seismogram as discrete arrivals: we use the ratio of the peak amplitude outside the

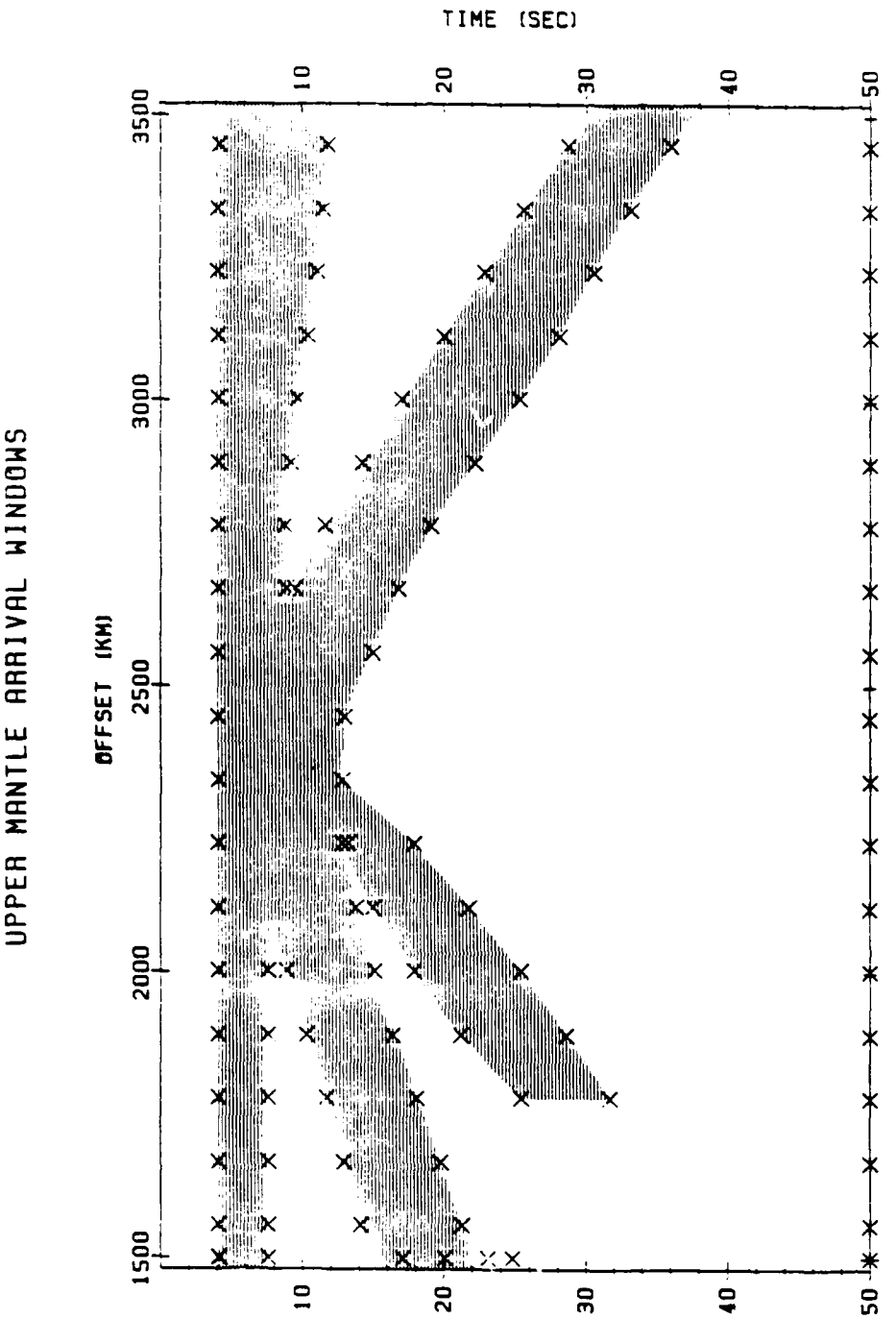

Figure 18. Arrival windows for upper mantle phases.

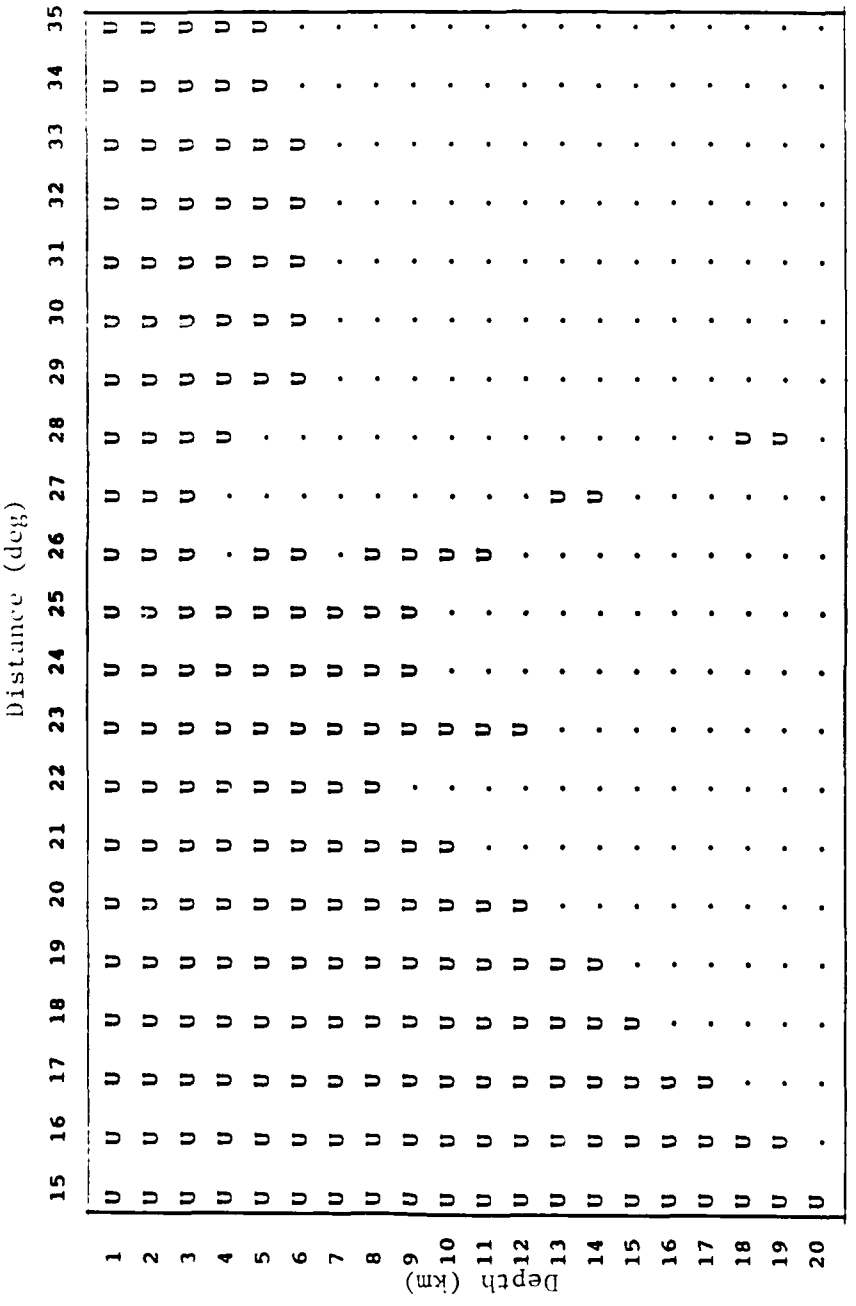

Figure 19. Depth resolution of methods that require identification of pP source depth or source mechanism determination.

arrival windows to the peak amplitude inside the windows, up to some maximum time that is determined by the possible depth range of the event. As indicated in Figure 20a, for 256 explosion seismograms recorded between 1000 and 3500 km, nearly 25% of the explosion records had peaks outside the windows that were greater than those inside, a percentage that seemed excessively high.

Figure 20b shows a histogram that illustrates the distances at which the complexity model fails. On closer examination of the explosion results, a set of 36 traces recorded at the NORSAR array elements stands out. 29 of these 36 traces, shown in Figure 21, show high amplitudes outside of the upper mantle arrival windows and late in the records. A similar phenomenon can be observed in Figure 2 of King and Calcagnile (1976). The local structure underneath the NORSAR array is unlikely to be the cause because a second event, shown in Figure 22, has no traces showing high amplitudes outside arrival windows. Seismograms recorded at GRFO for 3 different events at similar distances exhibit the same pattern of late, high amplitudes. This suggests that the first arrivals at these distances are being attenuated, relative to the coda. This is perhaps not too surprising since these observations are close to the ends of the two branches, P_{AB} and P_{CD}, and scattered and diffracted energy associated with these branches may be responsible for the apparently energetic coda. The synthetic results presented in Section 2 also show that the first arrival is predicted to be small relative to the coda at these

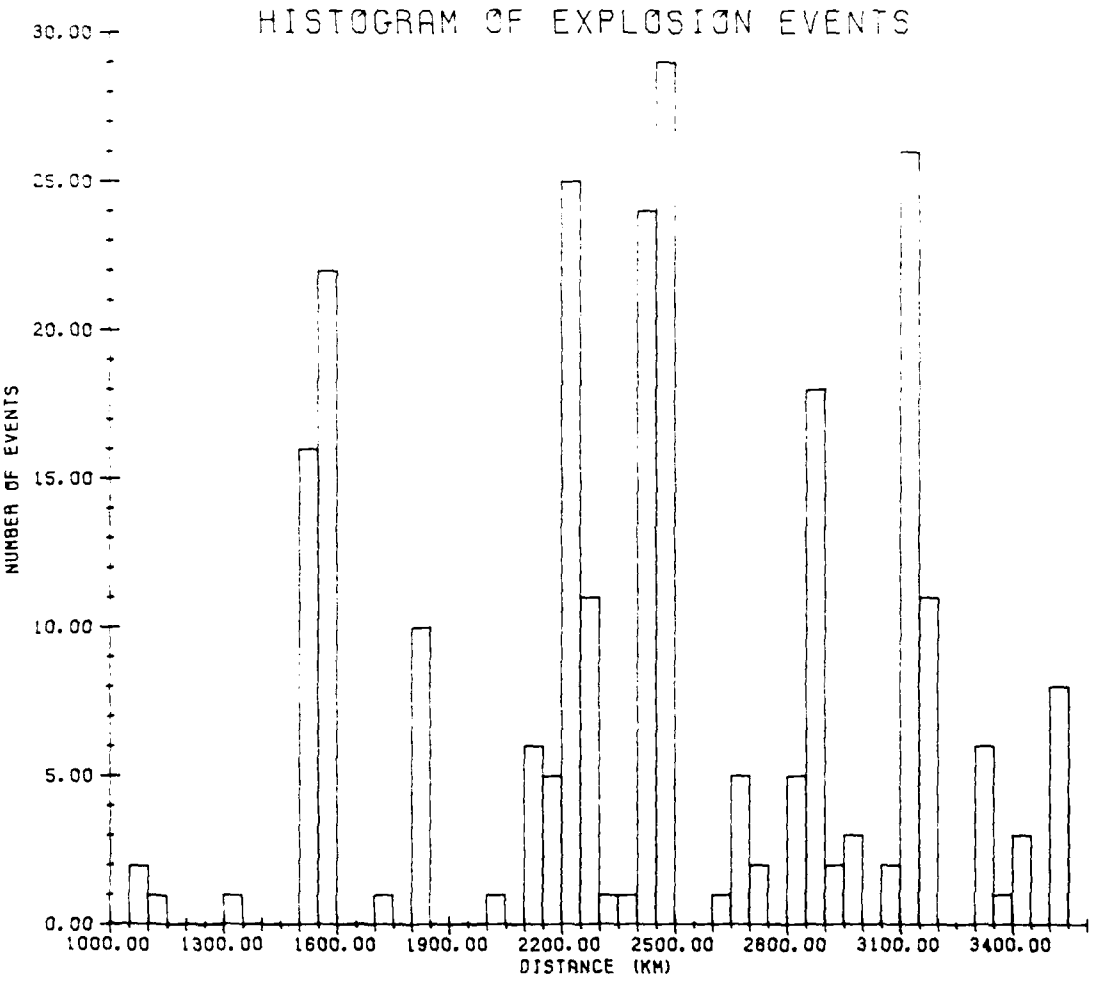

Figure 20a. Histogram of available digital seismograms from explosions in Northwest Eurasia, used to analyze complexity in waveforms recorded between 1000 and 3500 km.

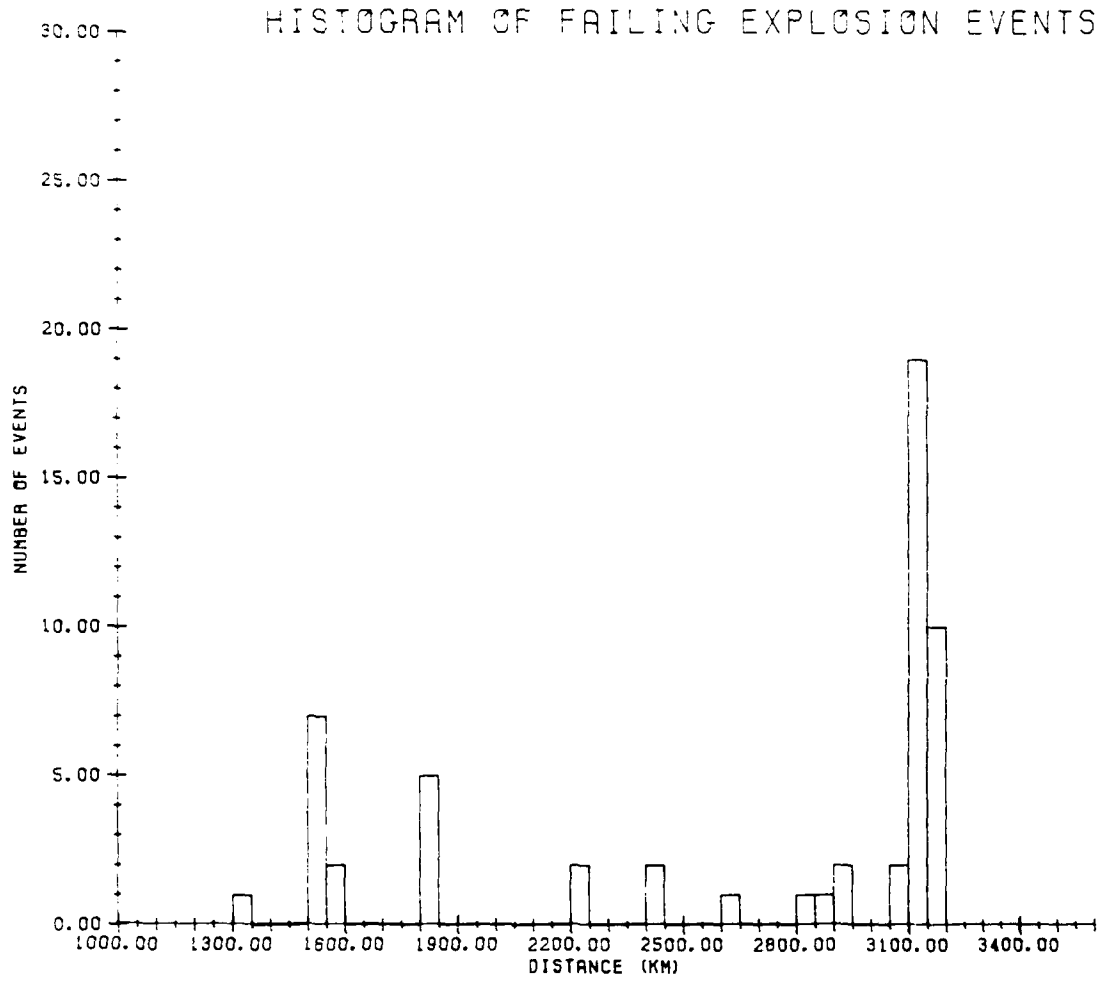

Figure 20b. Histogram showing the distribution with distance of those seismograms with large later arrivals (peak amplitudes) that do not correspond to predicted upper mantle arrivals.

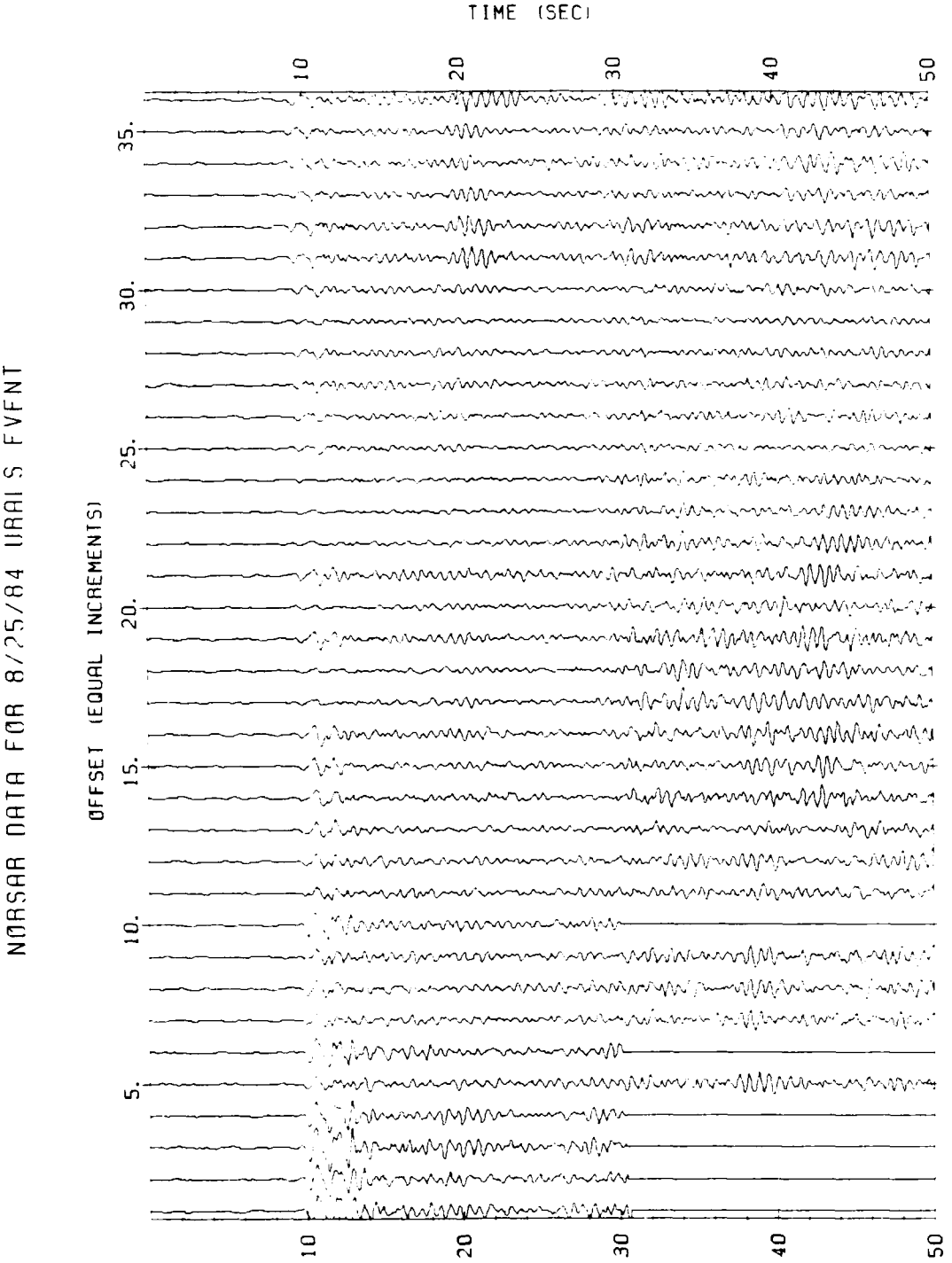

Figure 21. NORSAR array seismograms for Soviet PNE at 3160 km (to N1A0), 61° azimuth.

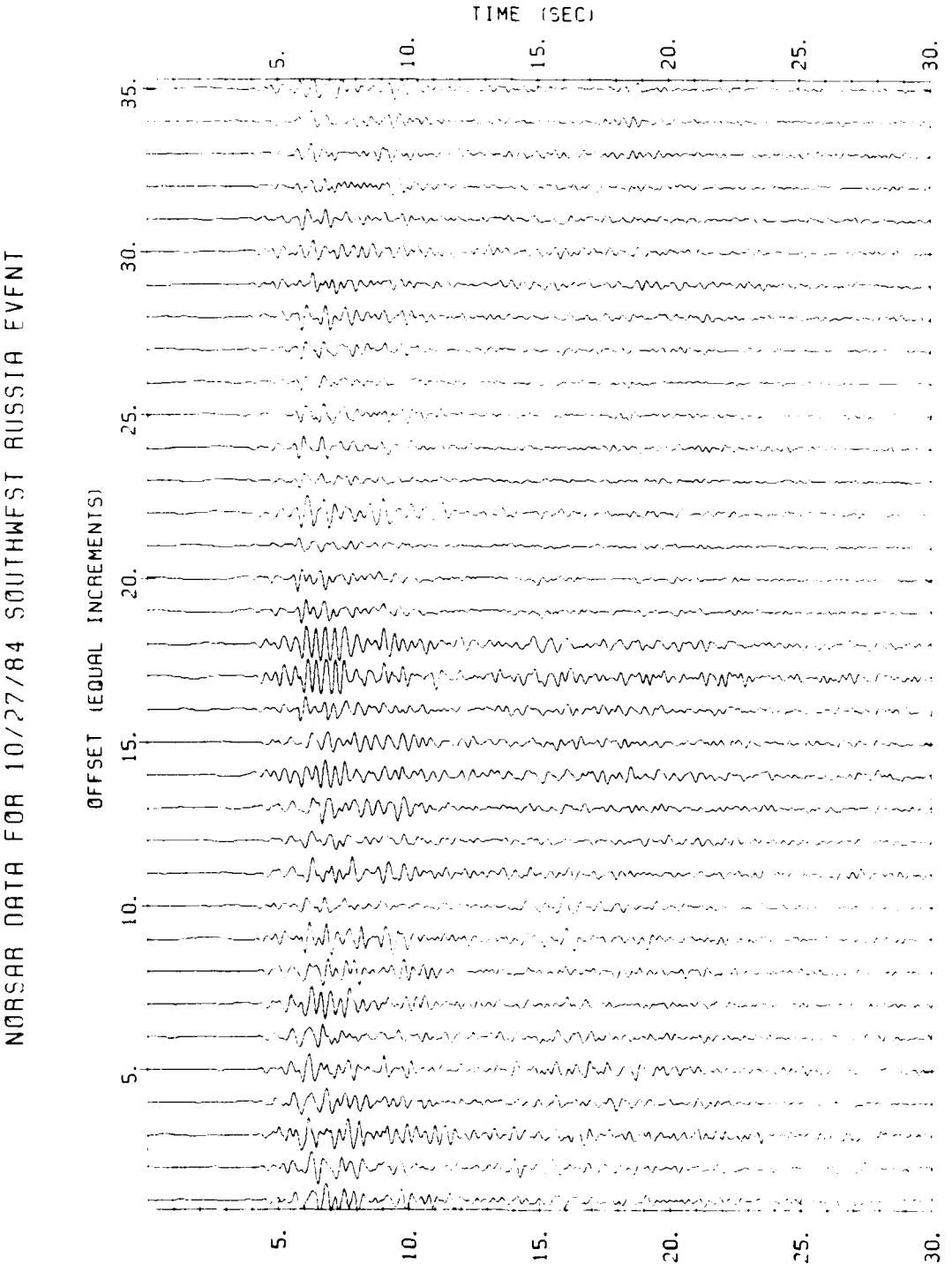

Figure 22. NORSAR array seismograms for Soviet PNE at 2844 km (to NIAO), 106° azimuth.

distances. Because of the relatively close proximity of NORSAR and GRFO, however, some azimuth effect can not be ruled out as a contributing factor.

Having noted this apparently "anomalous" distance, we re-computed the explosion results excluding the 42 traces in the distance range from 2900 to 3200 km. These new results indicate that only 10% of the explosion records have high amplitudes outside the upper mantle arrival windows. Although not a perfect score, this result is not unreasonable given the many sources for error. Most of the remaining problem data is at distances less than 2000 km. These include a sample of NORSAR data from an event at 1500 km, and some data recorded at KAAO from the Soviet test sites in East Kazakh. The KAAO data showed a large amplitude arrival between the initial P arrival, (P_{AB}) and P_{CD}, which was not included in our regionalization. The remaining discrepancies can be attributed to slight mis-alignment of the trace start times, overly restrictive upper mantle arrival windows, and poor signal to noise levels.

A similar experiment, using 168 array-summed earthquake seismograms from the NORESS array from shallow events at similar distances indicated that 45% of the data had arrivals outside the upper mantle windows that exceeded the amplitudes inside the windows. This result cannot be further evaluated since the depths and focal mechanisms of the events are unknown.

A complexity criterion for the 10 to 30 degree distance range that takes into account the times when upper mantle arrivals are expected provides observational evidence that the Pearce algorithm may be a useful discrimination tool at these distances, given the requisite azimuthal coverage. The above evaluation relies on a calibration procedure. Explosion data was used to determine the velocity structure and isolate the upper mantle arrival windows. We used a small sample of explosion data recorded at a few stations to extrapolate to what an explosion should look like at all distances in the region of interest. It remains to be seen whether earthquake data can be similarly used to calibrate a region.

5.0 Autocorrelation and Cepstral Analysis of Upper Mantle Seismograms

The complex nature of upper mantle seismograms makes utilization of the raw seismograms in locating depth phases difficult. If a convolutional model applies for upper mantle P-waves, the autocorrelation function is a useful device for separating upper mantle and depth phases. Peaks corresponding to the pP-P, sP-P, and sP-pP times should be consistent between stations when corrected for distance, while peaks corresponding to upper mantle triplications will vary in location depending on distance. If peaks corresponding to depth phases can be identified in the autocorrelation functions, then either a Pearce algorithm, or similar technique, can be used directly on the autocorrelation functions, or the derived delay times can be used in further processing and modeling of the raw seismograms.

Figure 23 illustrates a sample upper mantle seismogram and its autocorrelation function. Clearly, the band-limited nature of the correlation function, which spreads the zero-lag correlation peak, limits the utility of the autocorrelation function for the identification of depth phases for shallow events. Some form of spectral balancing (or pre-whitening) must be applied. Two forms of pre-whitening are compared in this work: replacing the autocorrelation function by the power cepstrum and extracting and deconvolving an effective wavelet from the autocorrelation function.

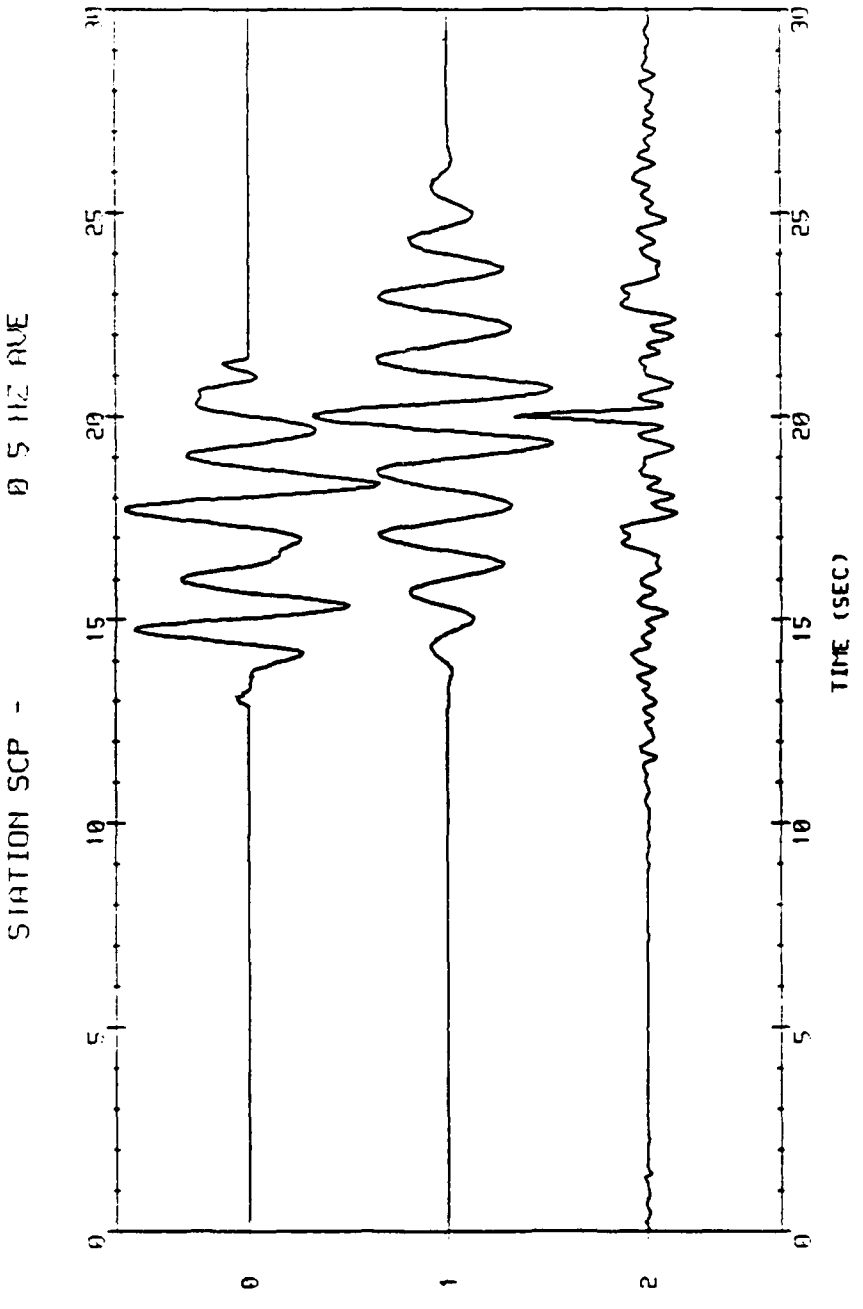

Figure 23. DWWSS SPZ seismograms recorded at station SCP from an event in Idaho on October 29, 1983.

The power cepstrum is the inverse Fourier transform of the logarithm of the power spectrum. Use of the logarithm has the effect of whitening the spectrum. In addition, the power cepstrum enhances the spectral holes that result from interference of depth phases. This latter feature is probably of little use in the range of ray parameters present in upper mantle seismograms because changes in pP times between branches can be as large as 5% of pP-P time. A change of a few tenths of a second in pP timing may have relatively little effect on the overall spectral shape at the frequencies of interest, but it can effectively eliminate spectral holes making cepstral estimates difficult to interpret.

An alternate form of pre-whitening is the application of a spiking filter to the autocorrelation function. We start with a simple convolutional model of the seismogram:

$$u(t) = s(t) * \Sigma \{ (e_i(t,p_i) * d_i(t,p_i) * q_i(t) \} \qquad (1)$$

where $s(t)$ is the source time function, $e_i(t,p_i)$ is the ith refracted arrival from the upper mantle with ray parameter (or slowness) p_i, $d_i(t,p_i)$ is the sequence of P, pP, and sP phases that have been refracted along the propagation path characterized by $e_i(t,p_i)$, and $q_i(t)$ is the attenuation function for the ith upper mantle arrival. To devise our spiking filter for the autocorrelation function, we make some additional simplifying assumptions to our convolutional model in Equation 1. One further assumption is that the difference in the attenuation between the different upper mantle branches is negligible.

This is justified by the work presented in Der et al. (1986) in which they determined the differential t* for the major branches of the upper mantle arrivals in western Eurasia. With this assumption, we can separate the frequency dependent part of Equation 1 into the effective source wavelet, $s_e(t)$, where

$$A(t) = s_e(t) \odot s_e(t) * k(t) \odot k(t). \qquad (2)$$

In Equation 2, A(t) is the autocorrelation function, k(t) is the spike wavetrain and $\odot$ indicates correlation. Our final assumption is that the windowed autocorrelation, $\hat{A}(t)$, windowed symmetrically about t=0, is an approximation of the autocorrelation of the effective source. This windowing is implemented in the frequency domain by smoothing the power spectrum, typically with a boxcar or exponential, and by dividing the original power spectrum by the result. Since the autocorrelation is zero phase, a suitable spiking filter may be expressed as:

$$f(\omega_o) = \int_{-\infty}^{\infty} W(\omega_o - \omega)\, P(\omega)\, d\omega$$

where W is a window function and P is the Fourier transform of the autocorrelation function. For this study a symmetric boxcar window function was used. The filtered correlation function used in this study is:

$$\hat{A}(\omega) = \frac{L(\omega)\, A(\omega)}{f(\omega) + \epsilon}$$

where L is a low-pass filter, and ϵ is a water level used to stabilize the deconvolution.

Figures 24-26 illustrate the use of the spiking filter on examples of an earthquake recorded at upper mantle distance. The data shown are from an aftershock of the 1983 Borah Peak, Idaho earthquake observed at distances ranging from 1700 to 2300. Note that while individual spike autocorrelations, shown in Figure 26, show a significant number of arrivals, only a few of these arrivals appear consistent from station to station. Autocorrelations in Figure 25 have been processed using a 0.5 Hz averaging window for the spiking filter, followed by a 3 Hz-corner low-pass filter to reject incoherent high frequency noise.

The autocorrelations show consistent arrivals at about 3 and 7 seconds. The coherent nature of these arrivals is illustrated by performing a time stretch to equalize moveout of depth phases with distance, enveloping, and stacking. The result, shown in Figure 27, enhances the arrivals at 3 and 7 seconds. A 3 second pP-P time corresponds well with the reported depth of 10 km. The nature of the 7 second arrival is not known.

Figure 28 illustrates the cepstra for this event. The stretched and stacked cepstrum, shown in Figure 29, once again shows arrivals at 3 seconds and 7 seconds. The agreement between these two methods lends some confidence that the observed coherent arrivals are not artifacts of the processing method used.

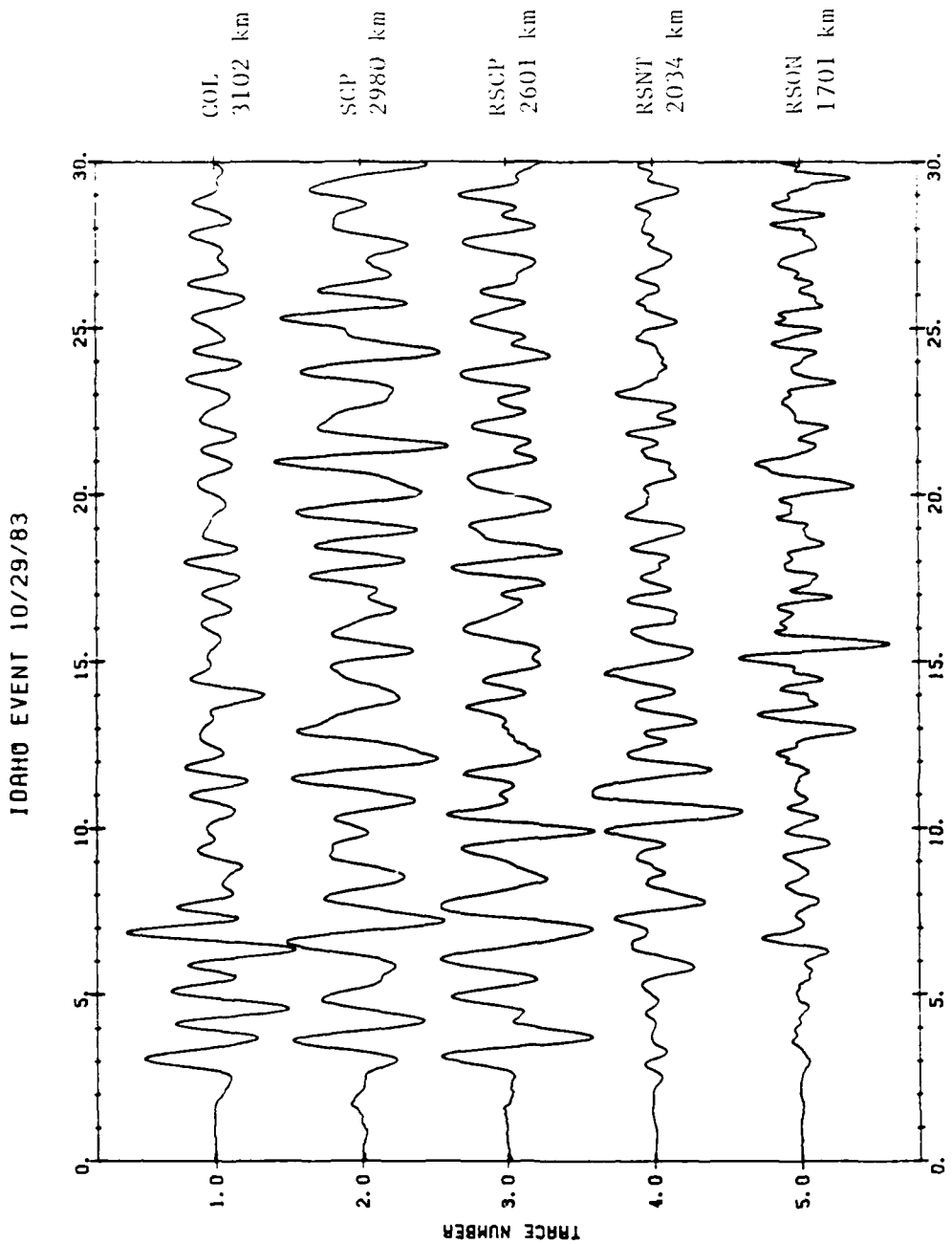

Figure 24. GDSN seismograms for the October 29, 1983 Idaho event.

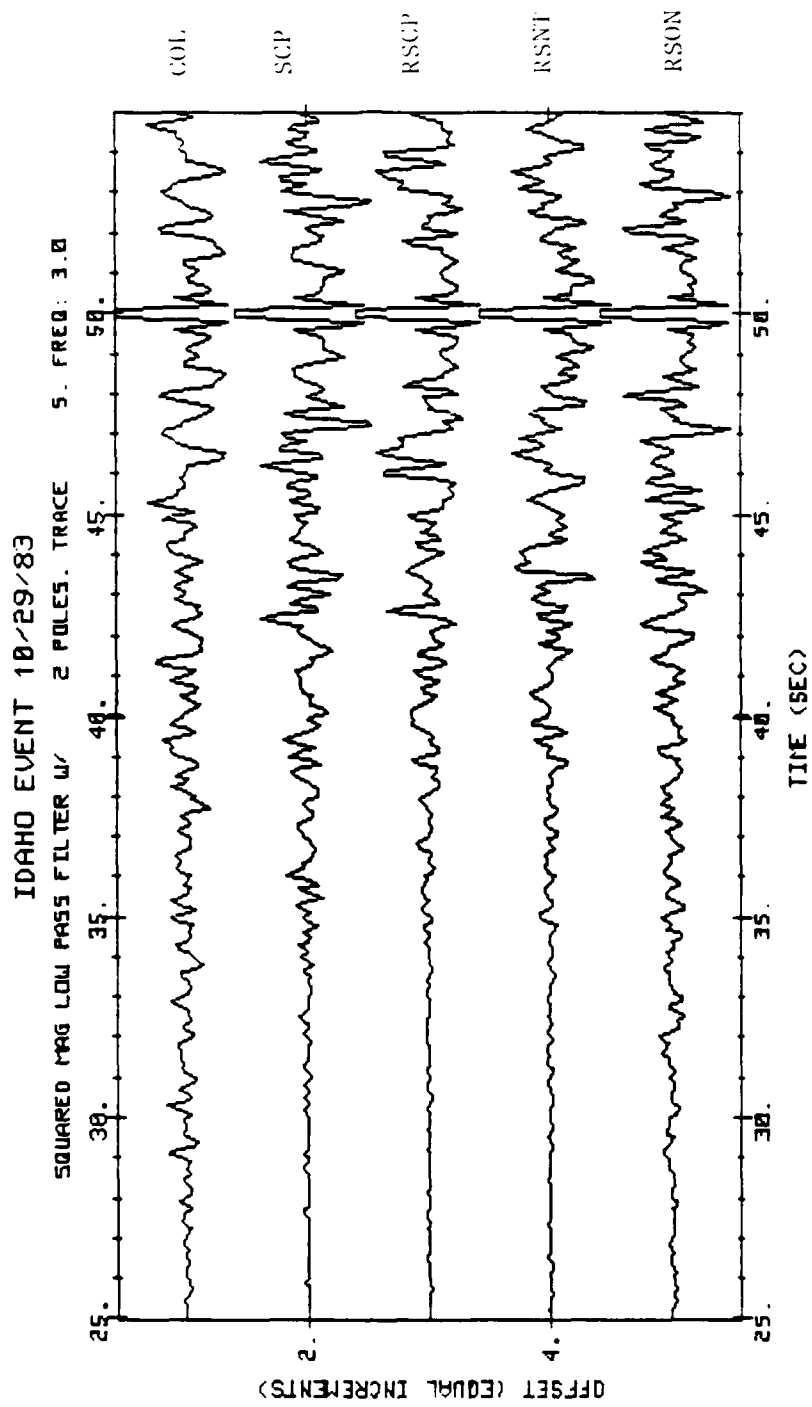

Figure 25. Spiked, filtered, autocorrelations of the seismograms shown in Figure 24.

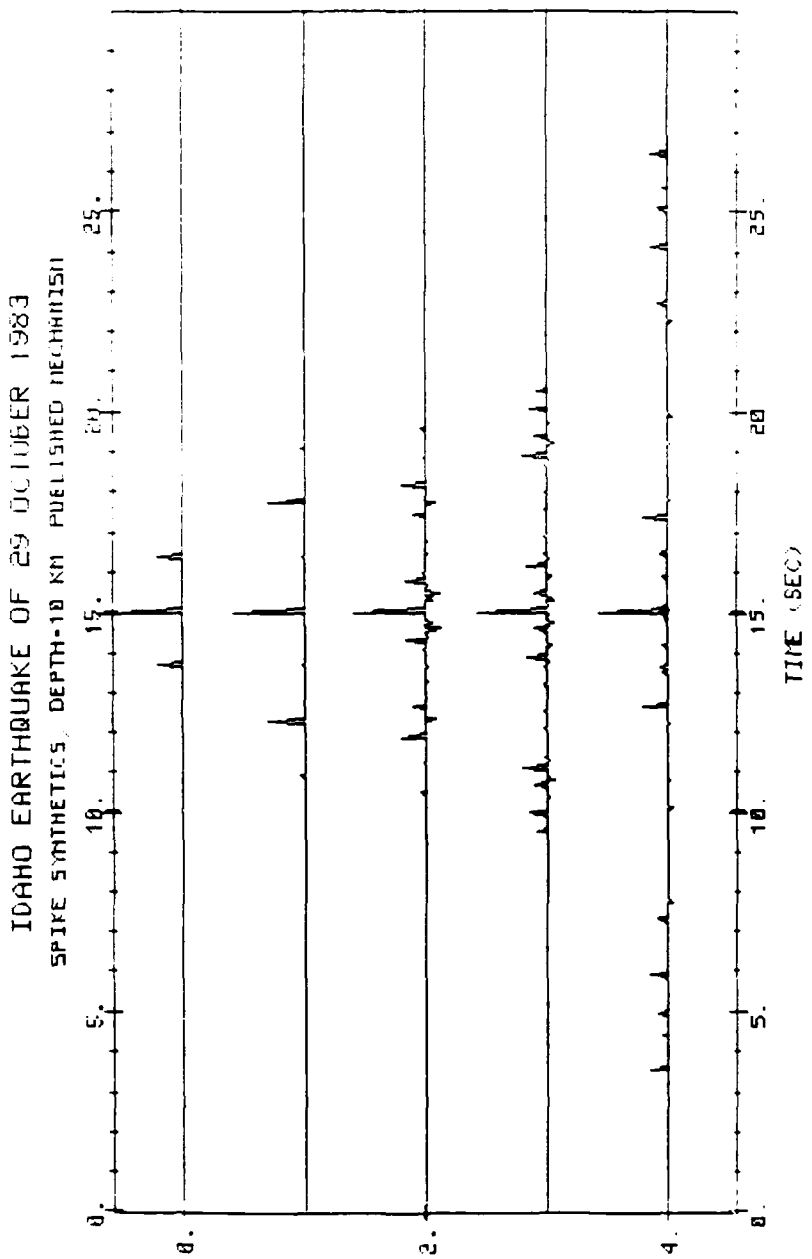

Figure 26. Autocorrelations of the spike seismograms for the Idaho event predicted using a published mechanism (Boatwright, 1985) and a source depth of 10 km.

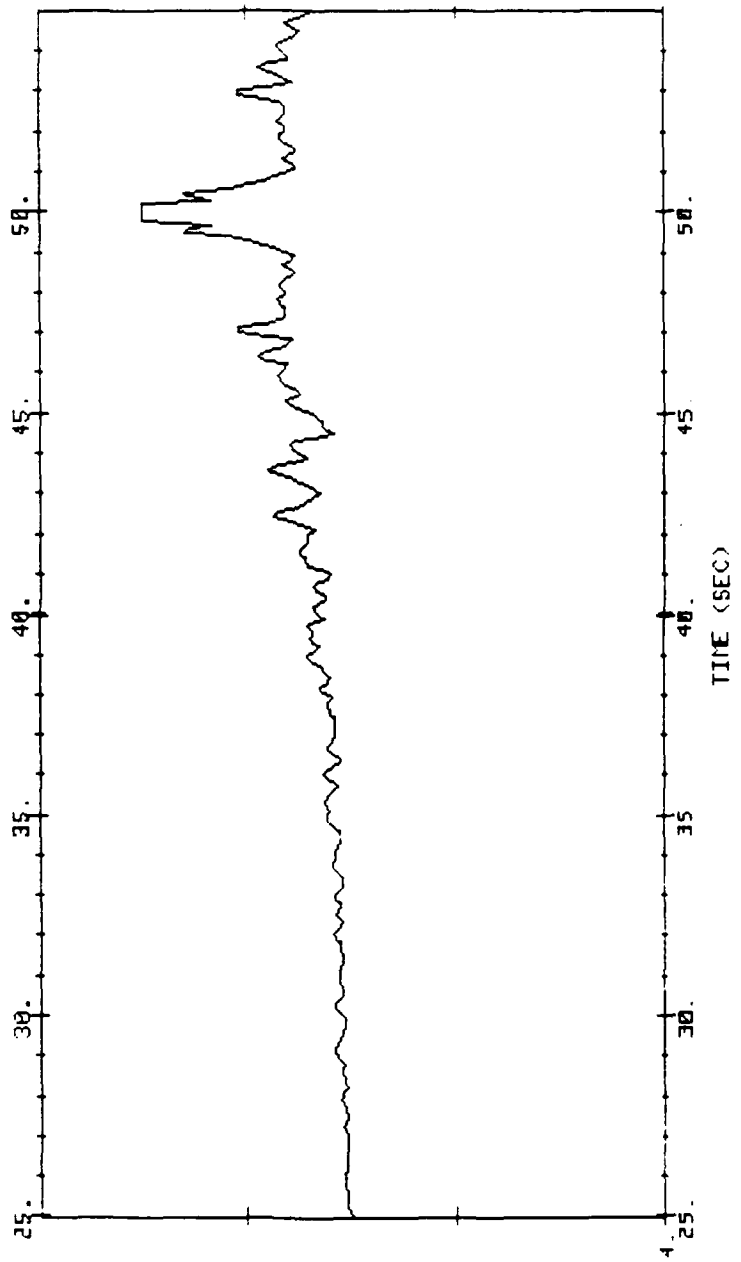

Figure 27. A stack of the envelopes of the filtered autocorrelation shown in Figure 25.

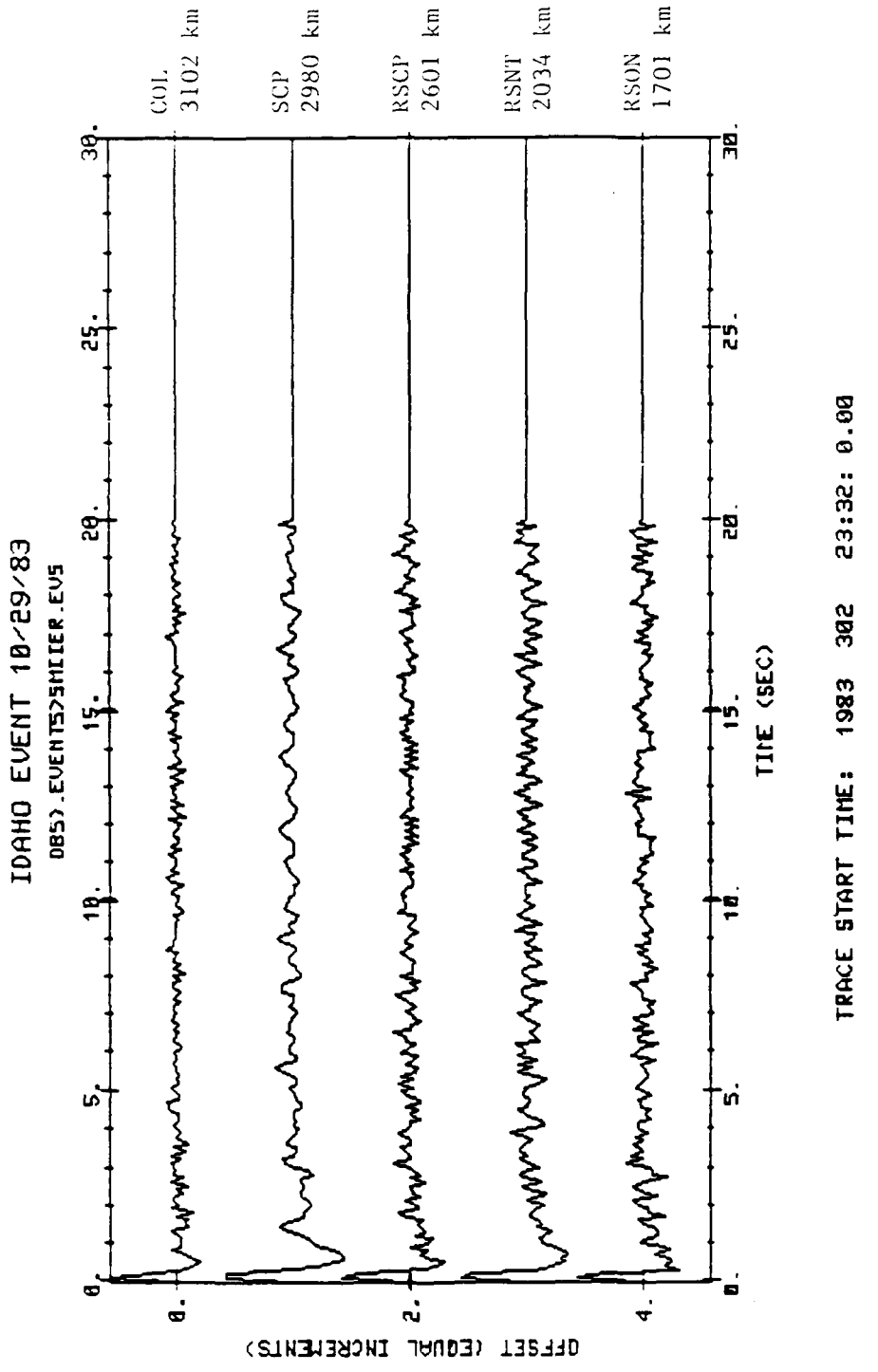

Figure 28. Power cepstra of the seismograms shown in Figure 24.

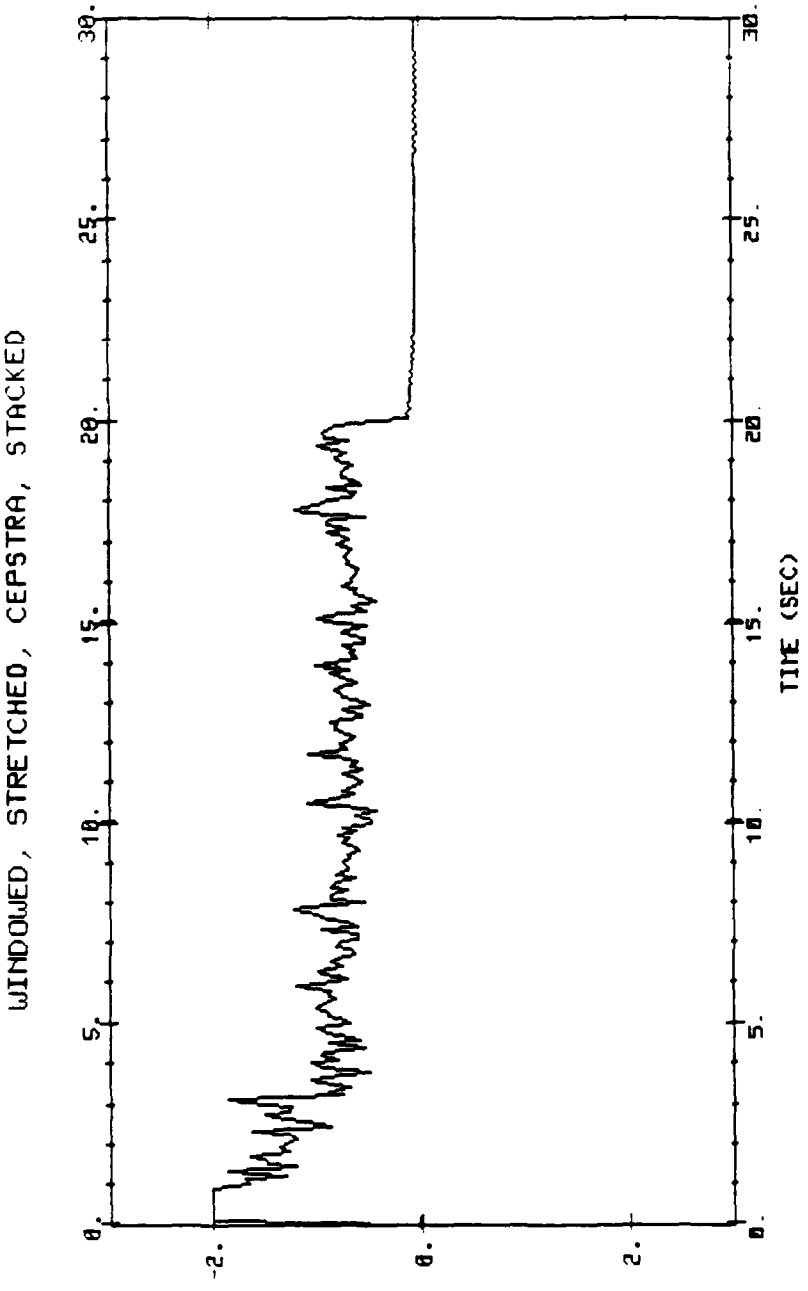

Figure 29. A stack of the envelopes of the power cepstra shown in Figure 28.

Initially, we had some optimism that meaningful polarity estimates could be extracted from the spiked autocorrelation functions. It did not prove any easier to observe polarity reversals on the processed autocorrelations than on the original seismograms. Unambiguous polarity estimates require good signal to noise properties over a wide frequency band, which is seldom the case for later arrivals at upper mantle distances.

6.0 Conclusions and Recommendations

This research has explored several avenues for using short period seismograms recorded at upper mantle distances for discrimination purposes. The focus of the research was on characterizing the time domain signature of seismograms from explosions and earthquakes and searching for discriminants that reflect physical differences between the two sources, such as depth and focal mechanism. Small events were of particular interest, which necessitated examining short period digital data. During this study, there was limited availability of short period data with good azimuthal coverage required to constrain focal mechanisms and depth. Thus most of our results are preliminary and our conclusions are limited by the availability of data.

Current upper mantle models for northwest Eurasia, with reasonably simple structures, are successful at predicting explosion seismograms from that region. The arrival times and relative amplitudes of the dominant phases can be accurately predicted and characterized. Nevertheless, there is always the possibility of the P-waves sampling a region of strong lateral heterogeneity, particularly near the source or receiver, and thus confidence in discrimination based on depth, source mechanism, or waveform complexity at a single station is small. A multiple station approach with complete azimuthal coverage is desired. Unfortunately, good coverage of the Soviet test sites of interest has not been available until very recently, and so, many of the ideas presented in this report could not be adequately evaluated.

Theoretical calculations of seismograms between 500 and 4000 km using the best available estimates of the velocity and attenuation structure suggest that, at frequencies between 1 and 2 Hz, the maximum amplitudes of the seismograms remain about constant between 750 and 2800 km. This result has implications for future network design and should be explored further using data more relevant to short period body wave propagation in the upper mantle.

Considerable effort was extended toward developing signal processing techniques to extract amplitude and polarity information from complex bandlimited waveforms using expected upper mantle models as constraints. The results of these studies were not promising. There appears to be significant differences in the amplitudes and phase of reflected phases, pP and sP that cannot be adequately described by the simple convolutional models that are assumed in the processing algorithms. We particularly sought information concerning polarity, since a clear reversal in polarity of a major later phase in the seismic waveform should be a powerful discriminant. However, coda levels at upper mantle distances are larger than typically observed at teleseismic distances. Polarity determination requires good signal to noise character over a broad range of frequencies, which is seldom the case at these distances.

A more promising area of research would involve developing ways to characterize observed complexity in seismograms at upper mantle distances and use a generalization of the Pearce algorithm as a basis for interpreting the observations. A major component of such an

approach is regional calibration of the upper mantle structure. This is possible in northwestern Eurasia due to large number of explosions from different regions. It is possible to estimate noise levels on which to base complexity measurements. A more difficult region might be one such as central Asia where little data has been recorded until recently. It is then necessary to calibrate the paths using earthquake data, which is much more difficult. One approach can be borrowed from the seismic exploration industry and involves slant stacking a large amount of data spread as much as possible over the range of distances of interest. The method relies on averaging to eliminate the effects of source depth and focal mechanism on the observations and hence requires substantial data recorded at several sites. The slant stack provides a convenient representation of the average seismogram at any distance with depth and focal mechanism removed and can be used as a reference against which to compare any complexity measurements of interesting events.

A major objection to complexity measurements that we are proposing is that they can obviously be confused by complex detonation patterns. There are good theoretical methods for detecting multiple sources (e.g. Flinn et al., 1973) however, there has been little evaluation of their effectiveness at regional distances. Any pursuit of complexity measurements would necessarily involve potential methods of deliberate evasion.

8.0 References

Apsel, R.J., 1979, Dynamic Green's functions for layered media and applications to boundary-value problems, Ph.D. Thesis, University of California, San Diego, 349 pages.

Apsel, R.J. and J.E. Luco, 1984, On the Green's function for a layered half space, Bull. Seism. Soc. Am. 73, 909-930.

Burdick, L.J. and D.V. Helmberger, 1979, The upper mantle P velocity structure of the western United States, J. Geophys. Res. 83, 1699-1712.

Chapman, C.H., 1978, A new method for computing synthetic seismograms, Geophys. J. R. Astr. Soc., 54, 481-518.

Der, Z.A., W.W. Chan, A.C. Lees and M.E. Marshall, 1986, Models of the frequency dependence of Q in the mantle underlying tectonic areas of North America, Eurasia and Eastern Pacific, TGAL 86-5, contract no. F08606-85-L-0023, Teledyne Geotech, Alexandria, Virginia

Douglas, A., 1967, P-wave signal complexity and source radiation patterns, VESIAC Report 7885-1-X, University of Michigan.

Douglas, A., 1981, Seismic source identification: a review of past and present research efforts, in Identification of Seismic Sources: Earthquake or Underground Explosion, E. Husebye and S. Mykkeltveit ed., D. Reidel: Dordrecht, Holland

England, P.C., M.H. Worthington and D.W. King, 1977, Lateral variation in the structure of the upper mantle beneath Eurasia, Geophys. J. R. Astr. Soc. 48, 71-79.

Flinn, E.A., T.J. Cohen, and D.W. McCowan, 1973, Detection and analysis of multiple seismic events, Bull. Seism. Soc. Am. 63, 1921-1936.

Given, J. W., and D.V. Helmberger, 1980, Upper mantle structure of northwest Eurasia, J. Geophys. Res. 85, 7183-7194.

Given, J.W., S.M. Ihnen, G.R. Mellman, and W.C. Tucker, 1987, Discrimination studies using seismograms recorded at upper mantle distances, Sierra Geophysics Annual Report SGI-R-8-136, DARPA contract F08606-86-C0014.

Kappus, M.E., A.J. Harding and J.A. Orcutt, 1987, To tau-p and back (abstract), EOS, 68, 1373.

King D.W. and G. Calcagnile, 1976, P-wave velocity in the upper mantle beneath Fennoscandia and Western Russia, Geophys. J. 46, 407-432

Langston, 1982, Aspects of Pn and Pg propagation at regional distances. Bull Seis. Soc. Am 72, 457-472

Lernar-Lam, A.L. and T.H. Jordan, 1983, Earth structure from fundamental and higher mode waveform analysis, Geophys. J. 75, 759-797.

McLaughlin, K.L., D.W. Rivers and M.A. Brennan, 1983, Pearce Focal Sphere analysis of explosion and earthquake mechanisms. TGAL-TR-83-4 contract no. F08606-79-C-0007; Teledyne Geotech, Alexandria, Virginia

McLaughlin, K.L., D.W. Rivers, M.E. Marshall and R.A. Wagner, 1985, Focal mechanism analysis as a method for teleseismic discrimination, in The Vela Program: A Twenty-Five Year Review of Basic Research, A.U. Kerr, ed. 735-740.

Pearce, R.G., 1977, Fault plane solutions using relative amplitudes of pP and P. Geophys. J. 50, 381-394.

Pearce, R.G., 1979, Earthquake focal mechanisms from relative amplitude of P, pP and sP: method and computer program, AWRE Report 0-41/79, Blacknest, Berkshire, England.

Pearce, R.G., 1980, Fault plane solutions using relative amplitudes of P and surface reflections: further studies. Geophys. J. 60, 159-157

Robinson, E. & S. Treitel, 1980, Geophysical Signal Analysis. Englewood Cliffs, N.J.: Prentice-Hall Inc.

Simpson, D.W., R.F. Merea, and D.W. King, 1974, Array study of P-wave velocities in the upper mantle transition zone beneath Northeastern Australia, Bull. Seism. Soc. Am. 61, 1751.

Smart, E. and K.L. McLaughlin, 1985, Discrimination by detection of the relative polarity of the entire P waveform. TGAL-85-12, contract no. FO 8606-85-C-0022, Teledyne Geotech, Alexandria, Virginia.

Thirlaway, H.I.S., 1966, Interpreting array records: explosion and earthquake P-wave trains which have traversed the deep mantle, Proc. R. Soc. Series A 290, 385-395.

Thorson, J.R. and J.T. Caerbout, 1985, Velocity-stack and slant-stack stochastic inversion, Geophysics, 50, 2727-2741.

Walck, M.C., 1984, The P-wave, upper mantle structure beneath an active spreading center: The Gulf of Calif., Geophys. J. 76, 697-724.

Walck, M.C., 1985, The upper mantle beneath the north-east Pacific Rim: a comparison with the Gulf of California, Geophys. J. R. Astr. Soc. 81, 243-276.

DISTRIBUTION LIST
FOR UNCLASSIFIED REPORTS
DARPA-FUNDED PROJECTS
(Last Revised: 15 Mar 88)

RECIPIENT	NUMBER OF COPIES
DEPARTMENT OF DEFENSE	
DARPA/NMRO ATTN: Dr. R. Alewine and Dr. R. Blandford 1400 Wilson Boulevard Arlington, VA 22209-2308	2
Defense Intelligence Agency Directorate for Scientific and Technical Intelligence Washington, DC 20340-6158	1
Defense Nuclear Agency Shock Physics Washington, DC 20305-1000	1
Defense Technical Information Center Cameron Station Alexandria, VA 22314	12
DEPARTMENT OF THE AIR FORCE	
AFGL/LWH ATTN: Mr. J. Lewkowicz Terrestrial Sciences Division Hanscom AFB, MA 01731-5000	1
AFOSR/NP Bldg. 410, Room C222 Bolling AFB, Washington, DC 20332-6448	1
AFTAC/DA (STINFO) Patrick AFB, FL 32925-6001	1
AFTAC/TT Patrick AFB, FL 32925-6001	3
AFWL/NTESG Kirkland AFB, NM 87171-6008	1

RECIPIENT	NUMBER OF COPIES

DEPARTMENT OF THE NAVY

NORDA
ATTN: Dr. J. A. Ballard
Code 543
NSTL Station, MS 39529 — 1

DEPARTMENT OF ENERGY

Department of Energy
ATTN: Mr. Max A. Koontz (DP-52)
International Security Affairs
1000 Independence Avenue
Washington, DC 20585 — 1

Lawrence Livermore National Laboratory
ATTN: Dr. J. Hannon, Dr. S. Taylor, and Dr. K. Nakanishi
University of California
P. O. Box 808
Livermore, CA 94550 — 3

Los Alamos Scientific Laboratory
ATTN: Dr. C. Newton
P. O. Box 1663
Los Alamos, NM 87544 — 2

Sandia Laboratories
ATTN: Mr. P. Stokes, Dept. 9110
P. O. Box 5800
Albuquerque, NM 87185 — 1

OTHER GOVERNMENT AGENCIES

Central Intelligence Agency
ATTN: Dr. L. Turnbull
OSI/NED, Room 5G48
Washington, DC 20505 — 1

U. S. Arms Control and Disarmament Agency
ATTN: Dr. M. Eimer
Verification and Intelligence Bureau, Rm. 4953
Washington, DC 20451 — 1

U. S. Arms Control and Disarmament Agency
ATTN: Mr. R. J. Morrow
Multilateral Affairs Bureau, Rm. 5499
Washington, DC 20451 — 1

RECIPIENT	NUMBER OF COPIES
OTHER GOVERNMENT AGENCIES (Continued)	
U. S. Geological Survey ATTN: Dr. T. Hanks National Earthquake Research Center 345 Middlefield Road Menlo Park, CA 94025	1
U. S. Geological Survey MS-913 ATTN: Dr. R. Masse Global Seismology Branch Box 25046, Stop 967 Denver Federal Center Denver, CO 80225	1
UNIVERSITIES	
Boston College ATTN: Dr. A. Kafka Western Observatory 381 Concord Road Weston, MA 02193	1
California Institute of Technology ATTN: Dr. D. Harkrider Seismological Laboratory Pasadena, CA 91125	1
Columbia University ATTN: Dr. L. Sykes Lamont-Doherty Geological Observatory Palisades, NY 10964	1
Cornell University ATTN: Dr. M. Barazangi INSTOC Snee Hall Ithaca, NY 14853	1
Harvard University ATTN: Dr. J. Woodhouse Hoffman Laboratory 20 Oxford Street Cambridge, MA 02138	1
Massachusetts Institute of Technology ATTN: Dr. S. Soloman, Dr. N. Toksoz, and Dr. T. Jordan Department of Earth and Planetary Sciences Cambridge, MA 02139	3

RECIPIENT	NUMBER OF COPIES
UNIVERSITIES (Continued)	
Southern Methodist University ATTN: Dr. E. Herrin and Dr. B. Stump Geophysical Laboratory Dallas, TX 75275	2
State University of New York at Binghamton ATTN: Dr. F. Wu Department of Geological Sciences Vestal, NY 13901	1
St. Louis University ATTN: Dr. O. Nuttli and Dr. R. Herrmann Department of Earth and Atmospheric Sciences 3507 Laclede St. Louis, MO 63156	2
The Pennsylvania State University ATTN: Dr. S. Alexander Geosciences Department 403 Deike Building University Park, PA 16802	1
University of Arizona ATTN: Dr. T. Wallace Department of Geosciences Tucson, AZ 85721	1
University of California, Berkeley ATTN: Dr. T. McEvilly Department of Geology and Geophysics Berkeley, CA 94720	1
University of California, Los Angeles ATTN: Dr. L. Knopoff 405 Hilgard Avenue Los Angeles, CA 90024	1
University of California, San Diego ATTN: Dr. J. Orcutt Scripps Institute of Oceanography La Jolla, CA 92093	1
University of Colorado ATTN: Dr. C. Archambeau CIRES Boulder, CO 80309	1

RECIPIENT	NUMBER OF COPIES
UNIVERSITIES (Continued)	
University of Illinois ATTN: Dr. S. Grand Department of Geology 1301 West Green Street Urbana, IL 61801	1
University of Michigan ATTN: Dr. T. Lay Department of Geological Sciences Ann Arbor, MI 48109-1063	1
University of Nevada ATTN: Dr. K. Priestley Mackay School of Mines Reno, NV 89557	1
University of Southern California ATTN: Dr. K. Aki Center for Earth Sciences University Park Los Angeles, CA 90089-0741	1
DEPARTMENT OF DEFENSE CONTRACTORS	
Analytical Sciences Corporation, The Dr. Richard Sailor ATTN: Document Control 55 Walkers Brook Drive Reading, MA 01867	1
Applied Theory, Inc. ATTN: Dr. J. Trulio 930 South La Brea Avenue, Suite 2 Los Angeles, CA 90036	1
Center for Seismic Studies ATTN: Dr. C. Romney and Mr. R. Perez 1300 N. 17th Street, Suite 1450 Arlington, VA 22209	2
ENSCO, Inc. ATTN: Mr. John R. Stevenson P. O. Box 1346 Springfield, VA 22151	1

RECIPIENT	NUMBER OF COPIES
DEPARTMENT OF DEFENSE CONTRACTORS (Continued)	
ENSCO, Inc. ATTN: Dr. R. Kemerait 445 Pineda Court Melbourne, FL 32940-7508	1
Gould, Inc. ATTN: Mr. R. J. Woodard Chesapeake Instrument Division 6711 Baymeadow Drive Glen Burnie, MD 21061	1
Maxwell Laboratories, Inc. S-CUBED Reston Geophysics Office ATTN: Mr. J. Murphy, Suite 1112 11800 Sunrise Valley Drive Reston, VA 22091	1
Pacific Sierra Research Corp. ATTN: Mr. F. Thomas 12340 Santa Monica Boulevard Los Angeles, CA 90025	1
Rockwell International ATTN: B. Tittmann 1049 Camino Dos Rios Thousand Oaks, CA 91360	1
Rondout Associates, Inc. ATTN: Dr. P. Pomeroy P. O. Box 224 Stone Ridge, NY 12484	1
Science Applications International Corporation ATTN: Document Control (Dr. T. Bache, Jr.) 10260 Campus Point Drive San Diego, CA 92121	1
Science Horizons ATTN: Dr. T. Cherry and Dr. J. Minster 710 Encinitas Blvd., Suite 101 Encinitas, CA 92024	2
Sierra Geophysics, Inc. ATTN: Dr. R. Hart and Dr. G. Mellman 11255 Kirkland Way P. O. Box 3886 Kirkland, WA 98124	2

RECIPIENT	NUMBER OF COPIES
DEPARTMENT OF DEFENSE CONTRACTORS (Continued)	
SRI International ATTN: Dr. A. Florence 333 Ravensworth Avenue Menlo Park, CA 94025	1
Teledyne Industries, Inc. Teledyne Geotech Alexandria Laboratories ATTN: Mr. W. Rivers 314 Montgomery Street Alexandria, VA 22314-1581	1
Woodward-Clyde Consultants ATTN: Dr. L. Burdick P. O. Box 93254 Pasadena, CA 91109-3254	1
NON-U.S. RECIPIENTS	
Blacknest Seismological Center ATTN: Mr. Peter Marshall Atomic Weapons Research Establishment UK Ministry of Defense Brimpton, Reading RG7-4RS United Kingdom	1
National Defense Research Institute ATTN: Dr. Ola Dahlman Stockholm 80, Sweden	1
NTNF NORSAR ATTN: Dr. Frode Ringdal P. O. Box 51 N-2007 Kjeller Norway	1
OTHER DISTRIBUTION	
To be determined by the project office	0
TOTAL	81

END

6-89

DTIC